UQAR

Université du Québec
à Rimouski

ÉTUDE, SIMULATION ET CONTRÔLE D'UN SYSTÈME D'ÉNERGIES RENOUVELABLES INTÉGRANT UNE ÉOLIENNE, DES PANNEAUX SOLAIRES ET UNE GÉNÉRATRICE AU BIODIESEL

Mémoire présenté

dans le cadre du programme de maîtrise en ingénierie

en vue de l'obtention du grade de maître en sciences appliquées (M.Sc.A.)

PAR
© **SIELLE MARTIN SORO**

Août 2017

Composition du jury :

Jean-François-Méthot, président du jury, Université du Québec à Rimouski

Ahmed Chebak, directeur de recherche, Université du Québec à Rimouski

Ahmed Chériti, examinateur externe, Université du Québec à Trois-Rivières

Dépôt initial le 04/05/2017   Dépôt final le 21/08/2017

UNIVERSITÉ DU QUÉBEC À RIMOUSKI
Service de la bibliothèque

Avertissement

Je dédie ce mémoire à l'éternel mon Dieu pour toutes les grâces dont il a comblé ma famille. Nous le prions de nous aider à contribuer à un monde meilleur.

REMERCIEMENTS

S'il est vrai que lorsque l'on a pour soit la détermination, il est difficile de ne pouvoir parvenir à atteindre des objectifs fixés, force est aussi de reconnaitre que sans contribution extérieure, certaines grandes ambitions de l'homme restent au stade de projet. C'est pourquoi, je voudrais remercier et exprimer ma profonde gratitude à mon directeur de mémoire M. Ahmed Chebak pour sa disponibilité et son support sans faille dans la réalisation du présent mémoire. Mes remerciements vont aussi à la direction de l'UQAR qui a mis tous les moyens logistiques et didactiques à notre disposition afin de pouvoir réaliser nos travaux de recherche.

Je ne peux manquer d'adresser également mes sincères remerciements à la famille Coulibaly Soropiu qui m'a accueilli ici au Canada, et qui m'a aidé également dans mon intégration à cette nouvelle société québécoise. J'ai aussi une pensée très spéciale à mon oncle Monsieur Soro Dohoba à Abidjan en Côte d'Ivoire qui m'a appris les choses de la vie et qui m'a surtout motivé dans mon processus d'immigration au Canada. Je ne peux oublier d'adresser mes vifs remerciements à mon père Monsieur Soro Tiepéré Robert et à ma mère Tuo Soro pour leurs bénédictions abondantes.

Je ne peux conclure ce chapitre très important sans adresser un remerciement très spécial à ma petite famille, avec qui je partage mon quotidien, mon épouse Sylla Aminata et mes bébés Soro Elisé et Soro Yohann.

x

RÉSUMÉ

Le réchauffement climatique progresse d'année en année. Il est démontré par les scientifiques que les énergies fossiles en sont responsables. Celles-ci sont couramment utilisées par les populations pour leurs besoins. C'est pourquoi nous voulons sensibiliser les populations par l'enseignement sur les technologies des énergies renouvelables qui sont capables de lutter efficacement contre ce fléau.

Le but de ce travail de recherche est donc d'étudier le fonctionnement et le contrôle optimal d'un système hybride d'énergies renouvelables composé d'une éolienne, de panneaux solaires, d'une génératrice au biodiesel ainsi que d'une batterie de stockage. Ce système sera ultérieurement implanté dans un laboratoire pour des fins éducatives. Dans la première partie de ce travail, le concept du laboratoire est présenté où les différents composants sont spécifiés. Le choix et le dimensionnement des sources d'énergies sont aussi effectués et leurs systèmes sont étudiés et simulés séparément puis couplés.

Ensuite, dans la deuxième partie, la modélisation, la simulation et le contrôle des systèmes de sources d'énergie sont réalisés. Des contrôleurs de type MPPT (Maximum Power Point Tracking) sont utilisés pour l'extraction des puissances maximales des éoliennes et des panneaux solaires. Le contrôle de vitesse spécifique (TSR) est utilisé pour l'éolienne et la méthode «Perturber et Observer (P&O)» pour les panneaux solaires. Le système de la génératrice au biodiesel est aussi décrit et la stratégie de couplage des trois sources est démontrée. Un contrôleur par hystérésis est utilisé pour le démarrage et l'arrêt de la génératrice. Celle-ci ne démarre uniquement que lorsque la batterie est complètement déchargée. Ainsi, elle alimente la charge et charge simultanément la batterie jusqu'à ce que celle-ci atteigne son niveau de charge maximal. Des scénarios sont appliqués au système afin de valider son fonctionnement.

Dans la dernière partie, l'extraction des puissances maximales des sources est améliorée en remplaçant les contrôleurs précédents par des contrôleurs intelligents basés sur la logique floue. L'étude réalisée montre que ces contrôleurs permettent d'améliorer l'efficacité des éoliennes et des panneaux solaires. De plus, le couplage de trois sources assure la fiabilité du système hybride.

Mots clés : Système hybride, MPPT, logique floue, laboratoire éducationnel, énergie solaire, énergie éolienne.

ABSTRACT

The global climate warming has been progressing for decades. It has been demonstrated by scientists that fossil fuels are largely responsible for this scourge. The fossil fuels are commonly used by the population for their daily needs. That is the reason why we have found it useful to raise awareness of the harmful effects of fossil fuels and the usefulness of renewable energies that are capable of effectively fighting against fossil fuels progress. The purpose of this project is therefore to study a renewable energy hybrid power system composed of wind turbines, solar panels and a biodiesel generator as well as a storage battery which will be subsequently installed in a laboratory for educational purposes. To carry out our study, in the first part, the concept of the laboratory was presented which includes all the physical and software components that will be used in the laboratory. The choice and the sizing of the energy sources, the battery and the loads were performed and then studied separately and coupled. Then, in the second part, the modeling and the simulation of the energies sources were realized. MPPT controllers were used to extract maximum power from wind turbines and solar panels. The tip speed ratio (TSR) MPPT was used for the wind energy system and the Perturb and Observe (P&O) MPPT for the solar photovoltaic system. The biodiesel generator system was described and the coupling strategy of the three sources was then demonstrated. A hysteresis controller is used to start and stop automatically the biodiesel generator which only starts when the battery is fully discharged. Some scenarios were applied to the hybrid system to study its operation. In the last part, the extraction of the maximum power of the sources was improved by replacing the TSR and P&O controllers by intelligent controllers using the fuzzy logic. The study showed that the efficient controllers made it possible to improve the efficiency of wind turbines and solar panels. In addition, the coupling of three sources ensures the reliability of the hybrid system.

Keywords: Hybrid power system, fuzzy logic, MPPT, educational laboratory, solar energy, wind energy.

TABLE DES MATIÈRES

LISTE DES TABLEAUX

LISTE DES FIGURES

LISTE DES ABRÉVIATIONS, DES SIGLES ET DES ACRONYMES

AC	Alternative current
ANN	Artificial neural network
BDG	Biodiesel generator
COA	Center of area, centre de gravité
DC	Direct current
FL	Fuzzy logic
HCS	Hill-climb Search
HPS	Hybrid power system
ICT	Information and communication technologies
IP	Internet protocol
LAN	Local area network
MCM	Max Criterion Method
MPP	Maximum power point
MPPT	Maximum power point tracking
NN	Neural network
P&O	Perturbation et Observation

PMSG	Permanent magnet synchronous generator
PSF	Power Signal Feedback
SOC	State of Charge
SPV	Solar photovoltaic
TSR	Tip Speed Ratio
VPN	Virtual Private Network
WECS	Wind energy conversion system
WT	Wind turbine

LISTE DES SYMBOLES

A	Facteur idealizing
$°C$	Degré Celsius
CE	Changement de l'erreur
Cp	Coefficient de puissance
D	Rapport cyclique
dD	Variation du rapport cyclique
dP/dV	Pente entre la puissance et la tension du panneau solaire
$E(k)$	Pente entre la puissance et la tension du panneau solaire
G	Radiation solaire
I_{bat}	Courant de la batterie
I_{batmax}	Courant de charge maximale de la batterie
I_{dcR}	Courant de sortie du redresseur de la turbine éolienne
I_{FAV}	Courant continu moyen
I_{FRMS}	Valeur efficace du courant

I_{gen}	Courant de sortie du générateur
I_{load}	Courant de la charge
I_{mp}	Courant à la puissance maximale du panneau solaire
I_{out}	Courant de sortie de l'éolienne
I_{ph}	Courant photonique
I_{pv}	Courant de sortie du panneau solaire
I_{refout}	Courant de sortie de référence
I_s	Courant de saturation
I_{sc}	Courant de court-circuit
I_{wind}	Courant de sortie de la turbine éolienne
K	Instant d'échantillonnage
$°K$	Degré Kelvin
K	Constant de Boltzmann's (1.38x10-23 J/K)
K_i	Coefficient température du courant
K_v	Coefficient température de la tension
$N_{oct}(°C)$	Température nominale de la cellule en degré Celsius
N_s	Nombre de cellules
P_{hyb}	Puissance de l'énergie hybride éolienne et solaire

P_{load}	Puissance de consommation de la charge
P_{mp}	Puissance maximale du panneau solaire
P_{net}	Puissance nette (différence entre puissance de l'hybride et de consommation de la charge)
P_{opteol}	Puissance optimale de l'éolienne
P_{spv}	Puissance de sortie du système de conversion de l'énergie solaire
P_{wt}	Puissance de sortie du système de conversion de l'énergie éolienne
Q	Capacité de la batterie
q	Charge électrique (1.6x10-19 Coulombs)
R	Longueur de la pale
R_s	Résistance série
Rsh	Résistance shunt
T	Température
T	Température absolue de la cellule
U_{out}	Tension de sortie de l'éolienne
V_{dc}	Tension continue
V_{dcR}	Tension de sortie du redresseur de la turbine éolienne
V_{in}	Tension d'entrée du panneau solaire
V_{mp}	Tension à la puissance maximale du panneau solaire

V_{oc}	Tension de circuit ouvert
V_{out}	Tension de sortie du panneau solaire
V_{ref}	Tension de référence du panneau solaire
V_{RRM}	Tension inverse maximale répétitive
ω_{opt}	Vitesse angulaire optimale
β	Pitch angle
ρ	Densité de l'air
η	Rendement de l'éolienne
λ	Tip Speed Ratio
λ_{opt}	Tip Speed Ratio optimal
ΔT	Élévation de la température dans les conditions de fonctionnement standards
ω	Vitesse angulaire de la turbine éolienne

INTRODUCTION GÉNÉRALE

MISE EN CONTEXTE

Les énergies fossiles telles que le pétrole, le charbon et le gaz naturel sont en grande partie responsables du réchauffement climatique global auquel nous sommes confrontés aujourd'hui. De plus, elles provoquent graduellement la dégradation avancée de la couche d'ozone et causent beaucoup d'autres dégâts écologiques et de la vie humaine. Pourtant, ces énergies sont aussi indispensables pour la vie quotidienne des populations d'où leur exploitation massive. Elles sont donc menacées d'épuisement à court ou moyen terme, ce qui fait craindre une éventuelle pénurie dans le futur. Cette situation a donc suscité le développement des énergies renouvelables telles que le solaire, l'éolien et les biocarburants qui permettent d'assurer un développement durable. Parmi celles-ci, l'éolien et le solaire sont ceux qui ont les plus émergés jusqu'à occuper une place prépondérante sur le marché mondial. L'énergie éolienne et l'énergie solaire présentent plusieurs avantages. Elles sont renouvelables et donc plusieurs générations à venir pourront en bénéficier, leur exploitation ne produit pas de dioxyde de carbone (CO_2), ni d'autres gaz et elles ne nécessitent pas de carburant. De plus, elles ne produisent pas de déchets et ne constituent pas d'énergies risquées comme l'énergie nucléaire. En outre, ces énergies sont relativement moins chères parce que leurs ressources telles que les radiations solaires et le vent sont abondantes et disponibles partout dans le monde.

Plusieurs recherches ont été effectuées dans le développement des énergies renouvelables afin de pallier les insuffisances de celles-ci notamment au niveau de leur caractère aléatoire. Ainsi, le couplage des éoliennes et des panneaux solaires s'est avéré une solution adéquate pour l'amélioration de la fiabilité des énergies renouvelables. Dans le cadre de notre projet, nous nous sommes orientés vers un système hybride qui va au-delà du couplage de deux sources d'énergie. Il est constitué de trois sources composées d'une

éolienne, de panneaux solaires et d'une génératrice au biodiesel dans le but de garantir la fiabilité de l'énergie renouvelable. Ce système sera étudié puis implanté à l'Université du Québec à Rimouski pour la formation des étudiants.

PROBLÉMATIQUE

Les panneaux solaires et les éoliennes utilisent respectivement les radiations solaires et le vent comme combustible pour fournir de l'énergie électrique. Cependant, les conditions météorologiques ont un impact majeur sur leur rendement. En effet, les panneaux solaires, d'une part, utilisent les radiations solaires pour fournir de l'énergie électrique; alors que ces dernières sont très variables au gré de la journée et des saisons. De plus, les panneaux solaires sont des systèmes non-linéaires qui ne fonctionnent pas toujours à leur point de fonctionnement maximal, ce qui résulte en des pertes d'énergie. D'autre part, les éoliennes utilisent le vent pour produire de l'énergie électrique; alors que le vent est aussi variable au gré de la journée et des saisons. À l'instar des panneaux solaires, les systèmes éoliens sont des systèmes non-linéaires qui ne fonctionnent pas toujours à leur point de fonctionnement optimal, ce qui provoque également des pertes d'énergie. Par ailleurs, les éoliennes et les panneaux solaires sont confrontés à une autre problématique majeure qui est celle de leur fiabilité vu leur caractère aléatoire.

i)   Efficacité des panneaux solaires

Dans la littérature, plusieurs travaux ont été déjà menés pour trouver les voies et les moyens pour contraindre les panneaux solaires à fonctionner aux points de fonctionnement optimaux afin d'augmenter leur productivité et leur efficacité. Cette technique est appelée la poursuite du point de puissance maximale (MPPT : Maximum Power Point Tracking). Ainsi, plusieurs algorithmes de commande de type MPPT ont été développés. Nous pouvons citer entre autres les plus populaires [1] : l'algorithme perturber et observer

(P&O), l'algorithme incrément de la conductance (INC), l'algorithme à base de la mesure d'une fraction de la tension *Voc* (FCO), l'algorithme à base de la mesure d'une fraction du courant *Icc* (FCC) et les algorithmes basés sur l'intelligence artificielle telle que la logique floue. Parmi ces algorithmes, l'algorithme P&O est l'un des plus utilisés dans le monde. Le principe de cet algorithme est d'effectuer une perturbation sur la tension du panneau solaire tout en agissant sur le rapport cyclique. En effet, suite à une perturbation, on calcule la puissance fournie par le panneau solaire à l'instant *k*, puis on la compare à la précédente puissance de l'instant (*k*-1). Si la puissance augmente, on s'approche alors du point à maximum de puissance (MPP Maximum Power Point) et la variation du rapport cyclique est maintenue dans le même sens. Au contraire, si la puissance diminue, on s'éloigne du MPP et le sens de la variation du rapport cyclique est inversé [2]. Cependant, cet algorithme présente des inconvénients décrits par M. Hatti [3]. Ce dernier a démontré que l'algorithme P&O présente des oscillations autour du point de puissance maximum, ce qui cause des pertes d'énergie, notamment dans le cas des systèmes photovoltaïques. En outre, il décrit un autre inconvénient du P&O en menant une étude sur un système photovoltaïque avec une variation brusque de l'ensoleillement. Il a pu observer que lorsqu'il y a une variation brusque de l'ensoleillement, la technique P&O continue à perturber le système dans la même direction alors qu'il est dans le mauvais sens provoquant une déviation du point de fonctionnement optimal. Ce phénomène affecte donc l'efficacité du système dans la mesure où il prend quelque temps supplémentaires pour se stabiliser. D'autres algorithmes plus intelligents et robustes ont été développés plus tard afin d'améliorer l'efficacité des panneaux solaires. Ces algorithmes sont basés sur les techniques de la logique floue et des réseaux de neurones artificiels. C'est la logique floue qui fera objet de notre étude dans ce projet. Cette technique a été développée par Lotfi Zadeh dans les années 1960. Elle se base sur la théorie des ensembles et vise à représenter les connaissances incertaines et imprécises, et fournit un moyen approximatif mais efficace pour décrire le comportement des systèmes qui sont trop complexes. Elle tente d'intégrer le

raisonnement et le savoir humain comme moyens pour la prise de décision. Ainsi, elle fournit une manière approximative mais néanmoins efficace pour la description du comportement des systèmes qui sont complexes à modéliser avec précision. Il en résulte des contrôleurs qui sont capables de prendre des décisions de contrôle intelligentes [4].

ii) Efficacité des éoliennes

La variation de la vitesse du vent affecte énormément l'efficacité et la productivité des éoliennes, d'où la nécessité de faire du contrôle. Dans la littérature, plusieurs techniques ont été développées entre autres : «Tip Speed Ratio (TSR) control», «Power Signal Feedback (PSF)», «Hill-Climb Search (HCS)», «Perturb and Observe (P&O)», etc. Parmi celles-ci, le contrôle de type TSR est l'une des méthodes les plus simples et les plus utilisées dans le monde. Cette technique consiste à maintenir le coefficient de puissance à son maximum afin de garantir un rendement maximum de la turbine. Cela correspond à trouver la vitesse spécifique qui maximise le coefficient de puissance. Cependant, la difficulté majeure est de trouver de façon précise cette vitesse spécifique qui dépend des caractéristiques de la turbine [5]. C'est pourquoi d'autres algorithmes intelligents plus robustes permettant de pallier les inconvénients des algorithmes précédemment cités ont commencé à émerger. Parmi ceux-ci, nous avons la logique floue et les réseaux de neurones artificiels [6]. Dans le cadre de notre projet, nous utiliserons la technique de la logique floue décrite précédemment.

iii) Couplage des sources d'énergie

Au-delà de la question de l'efficacité des systèmes d'énergie solaire et éolienne, les scientifiques se trouvent confrontés à un autre problème majeur, qui est celui de la fiabilité énergétique vu le caractère aléatoire du vent et de la radiation solaire. Pour tenter de résoudre ce problème, le couplage de deux sources d'énergies renouvelables s'est avéré

judicieux. Ainsi, plusieurs travaux ont été réalisés dans les technologies de couplage des énergies solaire et éolienne. M. Natsheh and A. Albarbar [7] ont proposé un système d'énergie hybride solaire et éolien avec stockage par batterie dans lequel ils utilisent un contrôleur de type logique floue pour faire fonctionner de manière optimum les sources d'énergie et le stockage. S. Kumar and V. K. Garg [8] ont aussi présenté un système d'énergie hybride solaire et éolienne avec stockage par pile à combustible dans lequel ils utilisent une unité d'alimentation en courant continu pour faire le couplage. Cependant, ces systèmes ne peuvent garantir une puissance continue vu que la vitesse de vent et les radiations solaires sont imprévisibles et de plus, l'énergie stockée dans les batteries ou dans les piles à combustible peut se trouver insuffisante dans certaines conditions. Pour remédier à ce problème, notre approche dans ce projet est d'intégrer une génératrice fonctionnant au biodiesel aux systèmes d'énergie solaire et éolienne pour constituer un système hybride à trois sources d'énergie. L'intérêt de l'utilisation du biodiesel, qui est également une source d'énergie renouvelable, est d'assurer la fiabilité du système. Ainsi, celle-ci sera utilisée comme une source secours dans les situations de mauvaises conditions météorologiques. Elle prendrait le relais automatiquement dans les conditions où l'énergie fournie par les éoliennes et les panneaux solaires n'est pas suffisante pour alimenter la charge dont les batteries ont été déchargées jusqu'à un certain seuil de charge (SOC) insuffisant. La génératrice au biodiesel va alors alimenter la charge et charger simultanément la batterie.

OBJECTIFS

L'objectif général de ce projet de recherche est d'étudier, de modéliser et de simuler un système d'énergie hybride intégrant l'énergie éolienne et solaire, une génératrice au biodiesel ainsi qu'une batterie de stockage. Ce système sera par la suite implanté physiquement dans un laboratoire pour des fins éducatives. Il s'agit aussi de développer le

contrôle optimal de chaque source d'énergie et de tout le système hybride. Les simulations sont effectuées à l'aide du logiciel Matlab/Simulink.

Les objectifs spécifiques consistent en l'étude séparée du fonctionnement et du contrôle du système de conversion d'énergie éolienne, du système solaire photovoltaïque et du système de la génératrice au biodiesel. Vu que les systèmes éolien et solaire sont des systèmes non-linéaires qui ne fonctionnent pas toujours de façon optimale, des techniques de poursuite des points de puissance maximale (MPP), et qui permettent d'augmenter leur productivité, sont conçues, simulées et analysées. Le fonctionnement du système hybride composé des trois sources d'énergies renouvelables et de la batterie de stockage est aussi étudié, validé et analysé. Pour ce faire, une stratégie de couplage est adoptée et la puissance produite par le système couplé en fonction des fluctuations du vent, de la variation de la radiation solaire et de la variation de la charge des batteries est simulée et analysée.

DÉMARCHE MÉTHODOLOGIQUE

Pour la réalisation de ce projet, trois phases sont adoptées. Dans la première phase, une étude préliminaire du système hybride d'énergies renouvelables composé du système éolien, du système solaire, de la génératrice au biodiesel ainsi que de la batterie de stockage est réalisée. En effet, les choix du type des panneaux solaires, de la turbine éolienne et de la génératrice au biodiesel ainsi que le dimensionnement de ces sources d'énergies, de la batterie de stockage et des charges à alimenter sont effectués. Les composants de l'électronique de puissance tels que les hacheurs et les redresseurs inclus dans le système hybride sont également dimensionnés. Les systèmes de puissance des différentes sources d'énergie considérées sont aussi étudiés et simulés séparément. En outre, dans cette phase, le concept du laboratoire éducationnel, où sera implanté le système hybride proposé, ainsi que son environnement physique et sa plateforme virtuelle (composants physiques et logiciels) sont présentés et expliqués.

Dans la deuxième phase du projet, une étude détaillée du fonctionnement du système hybride et de son contrôle optimal est effectuée. Ainsi, une modélisation des systèmes solaire et éolien est d'abord effectuée à l'aide d'équations mathématiques, puis les modèles développés sont simulés et analysés avec le logiciel Matlab/Simulink. Des contrôleurs MPPT sont intégrés dans ces deux systèmes afin d'extraire le maximum de puissance de l'éolienne et des panneaux solaires et d'assurer un contrôle optimal de ces systèmes. Pour cela, dans un premier temps, les techniques traditionnelles de poursuite du point de puissance maximale, qui sont les techniques P&O et TSR, sont utilisées respectivement dans le système solaire et le système éolien. Dans un deuxième temps, l'extraction des puissances maximales des sources est améliorée en remplaçant les contrôleurs TSR et P&O par des contrôleurs intelligents fonctionnant à l'aide de la technique de la logique floue afin d'augmenter l'efficacité et les performances des systèmes d'énergie éolienne et solaire. Le système de puissance de la génératrice au biodiesel est aussi modélisé, contrôlé et simulé.

Ensuite, la stratégie de couplage et de gestion de tout le système hybride est aussi démontrée. Ceci comprend les conditions de démarrage de la génératrice au biodiesel utilisée comme une source d'énergie secours dans le pire des scénarios tels que lorsque la vitesse de vent ou bien les radiations solaires sont très faibles ou encore lorsque les batteries sont complètement déchargées. Pour cela, un contrôleur par hystérésis est utilisé pour le démarrage et l'arrêt de la génératrice au biodiesel tout en maintenant la variation de l'état de charge de la batterie entre deux seuils minimal et maximal. Une étude du système hybride avec des scénarios suivant les variations de la vitesse du vent et des radiations solaires est, par la suite, effectuée afin d'analyser et de valider son fonctionnement et de comprendre l'intérêt de l'utilisation de trois sources d'énergie. Une comparaison entre les performances du système suivant l'utilisation du contrôle classique ou intelligent est aussi effectuée.

ORGANISATION DU MÉMOIRE

Ce mémoire est organisé sous forme d'articles. Il commence par une introduction générale qui débute par une mise en contexte du projet présentant le fléau du réchauffement climatique causé par les énergies fossiles, les enjeux des énergies renouvelables ainsi que le contexte du projet. La problématique liée aux systèmes d'énergies renouvelables, les objectifs à atteindre à travers ce projet de recherche et la méthodologie employée pour mener notre étude sont aussi présentés.

Trois articles ont donc été écrits dans le cadre de ce projet. Le premier article présente le concept d'un laboratoire d'énergies renouvelables dans lequel sera implanté le système d'hybride proposé ainsi que l'étude préliminaire de ce système et son dimensionnement.

Le deuxième article présente une étude par modélisation et simulation du fonctionnement et du contrôle du système hybride composé des sources d'énergie solaire et éolienne, de la génératrice au biodiesel ainsi qu'une batterie de stockage. Les techniques de contrôle de type TSR et P&O sont utilisés respectivement pour l'extraction de la puissance maximale dans l'éolienne et dans les panneaux solaires. Un système à hystérésis est utilisé pour le démarrage et l'arrêt de la génératrice au biodiesel utilisée seulement en secours lorsque l'état de charge (SOC) de la batterie est très bas. Le système est étudié suivant deux scénarios avec des conditions de variation de la vitesse du vent et des radiations solaires.

Le troisième article, quant à lui, présente une amélioration des techniques d'extraction des puissances maximales à l'aide de la technique de la logique floue. Une comparaison entre les résultats obtenus en utilisant les contrôleurs de la logique floue, d'une part, et le contrôleur P&O pour les panneaux solaires et le contrôleur TSR pour la turbine éolienne, d'autre part, est présentée.

Finalement, dans la dernière partie du mémoire, une conclusion générale du projet de recherche est présentée qui ressort l'importance du système proposé et des résultats obtenus et présente des recommandations pour les travaux de recherche à venir.

RÉFÉRENCES

[1]   H. Abbes and H. Abid, "Etude comparative de cinq algorithmes de commande MPPT pour un système photovoltaïque," International Journal of Control, Energy and Electrical Engineering, pp. 2356-5608, 2013.

[2]   A. Chermitti, O. Boukli-Hacene, and S. Mouhadjer, "Design of a Library of Components for Autonomous Photovoltaic System under Matlab /Simulink," International Journal of Computer Application, vol. 53, pp. 0975-8887, 2012.

[3]   M.Hatti, "Contrôleur Flou pour la Poursuite du Point de Puissance Maximum d'un Système Photovoltaïque," Jcge, 2008.

[4]   M. Azouz, A. Shaltout, and M. A. L. Elshafei, "Fuzzy Logic Control of Wind Energy Systems," International Middle East Power Systems Conference, 2010.

[5]   A. Karakaya, "Implementation of neural network-based maximum power tracking control for wind turbine generators," Turkish Journal of Electrical Engineering & Computer Sciences, vol. 22, pp. 1410-1422, 2012.

[6]   T.Shanthi and A.S.Vanmukhil, "Fuzzy Logic based MPPT Control of Hybrid Power Generation System," International Journal of Computer Application, vol. 86, pp. 0975-8887, 2014.

[7]   E. M. Natsheh and A. Albarbar, "Hybrid Power Systems Energy Controller Based on Neural Network and Fuzzy Logic," Smart Grid and Renewable Energy, vol. 4, pp. 187-197, 2013.

[8]   S. Kumar and V. K. Garg, "A hybrid model of solar-wind power generation system," International Journal of Advanced Research in Electrical, Electronics and Instrumentation Engineering vol. 2, pp. 2278-8875, 2013.

CHAPITRE 1

CONCEPT D'UN LABORATOIRE EDUCATIONNEL D'ÉNERGIES RENOUVELABLES INTÉGRANT L'ÉNERGIE SOLAIRE, ÉOLIENNE ET DU BIODIESEL

1.1   RESUME EN FRANÇAIS DU PREMIER ARTICLE

Cet article présente le concept d'un laboratoire éducationnel d'énergie renouvelable. L'objectif du laboratoire proposé est de permettre aux étudiants d'apprendre tous les aspects des énergies renouvelables et de faire une prise en main sur les équipements pour une meilleure compréhension des technologies de l'énergie propre. Ce laboratoire comprend un système hybride intégrant un système de conversion d'énergie éolienne, un système solaire photovoltaïque, une génératrice au biodiesel, des contrôleurs de suivi du point de puissance maximale et des batteries de stockage. Dans cet article, le dimensionnement des composants du système hybride est effectué et les trois systèmes de sources d'énergie renouvelables sont simulés et analysés séparément. Les panneaux solaires sont analysés sous des conditions de variation des radiations solaires et de température. Le fonctionnement du système est testé et analysé par une connexion directe à une batterie et à une charge résistive. Le système éolien est également analysé par une connexion directe à la batterie et à une charge résistive avec une vitesse de vent constante puis avec une vitesse de vent variable. En outre, la génératrice au biodiesel (BDG) équipée d'une machine synchrone à aimants permanents est simulée et analysée. Les trois sources d'énergie sont couplées et analysées avec des variations des entrées (radiations solaires, vitesse de vent). L'environnement physique du laboratoire est décrit et la plate-forme virtuelle est présentée.

Le concept de la formation en ligne et les sujets d'apprentissage dans le laboratoire ont également été abordés.

Le but de ce premier article était de présenter les composants du système hybride et de l'environnement du laboratoire d'énergies renouvelables où il sera implanté. Il s'agissait également d'analyser de façon succincte le fonctionnement des sources d'énergie, d'effectuer le choix et le dimensionnement de ces sources et des composants et de voir les résultats préliminaires du couplage des sources.

Ce premier article intitulé « Concept of Educational Renewable Energy Laboratory Integrating Wind, Solar and Biodiesel Energies » fut rédigé par moi-même. En tant que premier auteur, ma contribution à ce travail fut l'essentiel de la recherche sur l'état de l'art, le développement de la méthode et la rédaction de l'article. Le professeur Ahmed Chebak, second auteur, a fourni l'idée originale. Il a aidé à la recherche sur l'état de l'art, au développement de la méthode ainsi qu'à la révision de l'article. La première version de cet article a été présentée à la conférence « IEEE International Renewable and Sustainable Energy Conference » à Marrakech (Maroc) en Décembre 2015. Une version plus longue a été publiée en Décembre 2016 dans le journal « International Journal of Hydrogen Energy».

1.2 CONCEPT OF EDUCATIONAL RENEWABLE ENERGY LABORATORY INTEGRATING WIND, SOLAR AND BIODIESEL ENERGIES

ABSTRACT

This paper presents the concept of novel educational renewable energy laboratory. The proposed laboratory objective is to allow students to learn all aspects of renewable energies and take hands-on equipment's for better understanding of clean energy technologies. This laboratory includes a hybrid power system (HPS) integrating wind energy conversion system (WECS), solar photovoltaic (SPV), biodiesel generator, maximum power point tracking (MPPT) controllers and storage battery. In this paper, the whole HPS dimensioning is performed and the three renewable energy source systems are simulated and analyzed separately. The photovoltaic panels are examined under solar radiation and cell temperature variation conditions. The solar power functioning is verified and studied through a direct connection to battery and resistive load. The WECS is also analyzed through the same connection under constant wind's speed and variable wind's speed. Also, the biodiesel generator (BDG) using permanent magnet synchronous machine was simulated and analyzed. The three energy sources were coupled and analyzed under input parameters variations. The laboratory physical environment is described and the virtual platform is presented. The e-learning concept and the laboratory learning topics are also developed.

Keywords - hybrid power system; educational laboratory; renewable energies; remote laboratory; e-learning; wind and solar energies; maximum power point tracking.

1.3   INTRODUCTION

The world is now facing the global climate warming progress due to fossil fuels such as oil, coal and gas. All international organizations are taking necessary measures to fight against that issue. Renewable energies have been found as an alternative energy sources that allow building a sustainable development [1]. Among these renewable energies, solar and wind energy have become the most popular and widespread all over the world. Despite their development, solar and wind energies market penetration is still low. In fact, the wind and solar penetrations are respectively 30% and 10% [2].

To foster wind and solar technologies evolution and their teaching, development of renewable energy laboratories is to be considered. Herrera and Fuller have reported in [3] that laboratories are the center of science teaching and have a strong impact on students. However, traditional laboratories have shown some limits. Bauer and Mendes address this issue in [4]. They considered a situation in which specific experimental equipment is not offered by an institutional for students use. Eventually, a similar one is available and idle in a second institution, which could grant its remote use to the first one under proper agreements. Obviously, remote laboratory becomes a valuable solution to explore since it introduces many benefits such as: flexibility, maximal use, real experimentation and active learning [5].

Many researches were conducted in remote laboratory sciences in the past decades. Jara et al. presented in [6] a new collaborative e-learning system that allows a group of students to share experiences and at the same time their practice using Virtual Remote Laboratories (VRLs). That approach is very good since it allows teachers to track, supervise, and help students in their experimental exercises in a synchronous way. Fabregas et al. proposed in [7] a remote laboratory for engineering education using Simulink and EJS (Easy Java Simulink). Abdulwahed and Nagy presented in [8] a hybrid laboratory that incorporates three access mode (hands-on, virtual, remote) called Trilab using LabVIEW

and Joomla. All these authors developed new remote laboratory technologies for engineers so as to overcome traditional laboratories challenges. However, these remote laboratories were focused on systems such as three tanks and telerobotic systems, ball and hoop apparatus, etc. and did not address the issue with renewable energies. This paper focuses on providing an approach to the development of remote renewable energy laboratory for educational purposes. The renewable energy system implemented in this laboratory is a hybrid power system (HPS) with three energy sources. In general, a HPS consists of two or more energy sources systems, energy storage system, power conditioning equipment, and controllers [9]. The proposed system is based on the integration of wind, solar and biodiesel energy, storage battery, power conditioning system and coupling unit. That can not only help to reinforce researches on these energy sources but also sensitize students on the importance of clean energy. This study proposes a real physical renewable energy laboratory that is under construction at the Université du Québec à Rimouski (UQAR). The laboratory contains three renewable energy source systems: wind turbine, solar panel and biodiesel generator. A battery bank is used for energy storage. To generate renewable energies for testing purpose, a wind blower and variable insolation lamp are used. All critical data are measured and recorded in real time. These data includes but not limited to: wind's speed from wind blower, insolation lamp's light intensity, all system output voltage, current and power. The wind blower speed and the light intensity are variable.

This paper is organized as follows: the architecture and design of the hybrid power system are first presented. The solar power system, the wind energy conversion system (WECS) and the biodiesel generator are then studied respectively. The laboratory environment is also presented in terms of physical environment and virtual platform. Finally, the e-learning concept and the laboratory learning topics are developed.

1.4 HYBRID POWER SYSTEM

The HPS architecture considered for the laboratory is shown in Figure 1. It includes biodiesel generation system, solar power system, WECS, battery bank, DC-DC converters, rectifiers, inverter, and DC and AC loads that can vary. The proposed HPS is chosen to be based on three renewable energy sources (solar, wind and biodiesel) in order to ensure power reliability to loads. The solar and wind energies work as primary sources and the biodiesel generator as secondary source. Since the solar and wind energies depend respectively on sun radiation and wind speed, a power failure may occur in case of bad weather conditions (lack or low sun radiation and low wind speed). The backup biodiesel generator is set-up to take over the power supplying to charge the battery and feed the loads. So, the HPS is designed to assure power reliability in all conditions.
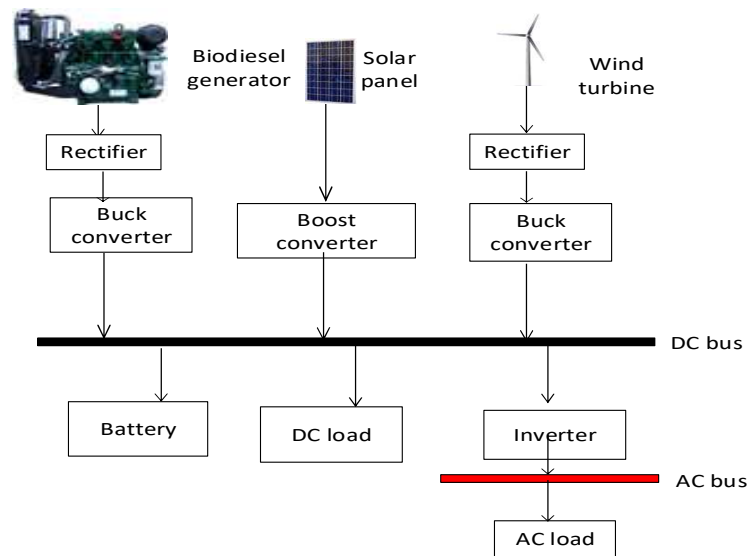
Figure 1. Hybrid power system architecture

We perform the dimensioning of all elements included in the proposed solution. Based on 300 W DC load, we choose 300 W wind power, 50 W solar panel and 400 W

biodiesel generator. Both solar panel and WECS are designed to feed the load simultaneously. Their nominal total power is 350 W that is 50 W higher than the DC load power because the power conversions loss between the sources and the load is taken into account to make sure that the power supply is enough. The battery bank is also dimensioned to store energy and supply power to the DC load. The biodiesel is used as backup and should be capable to feed the load itself when there is lack of solar and wind energies. As the DC load is 300 W, a 400 W generator is chosen taking into account the power conversion loss as well. One can notice that a 300 W AC load is also added in the HPS in order to operate the three energy sources systems at the same time and study their behavior in this case. The total capacity of the battery is chosen for 12 hours autonomy. The DC load energy consumption E_{load} for the 12 hours is calculated (in kWh) using the following equation

$$E_{load}[kWh] = P_{load}.Time \tag{1}$$

P_{load} is the DC load power and *Time* is the autonomy working time. For 300 W DC load power and 12 hours autonomy, the DC load energy consumption is 3.6 kWh.

Afterwards, the storage battery power capacity W_{bat} is calculated (in kWh) using the expression shown below. In this calculation, the battery conversion efficiency η_{bat} is taken into account and that is around 0.9.

$$W_{bat}[kWh] = {E_{load}}\Big/{\eta_{bat}} \tag{2}$$

Since the DC load energy consumption is 3.6 kWh, the calculated battery power capacity is 4 kWh.

The batteries sold in the market have standard voltage and capacity in Ampere-hour (Ah). So, we need to find the appropriate battery that can meet our requirements. A 24 V

battery is chosen where its power capacity (in Ah) is calculated from the following expression

$$W_{bat}[Ah] = 1000 \times \frac{W_{bat}[kWh]}{V_{bat}} \qquad (3)$$

V_{bat} is the battery voltage. As the needed battery power capacity calculated (in Ah) for 4 kWh and 24 V is 166.66 Ah, the 200 Ah is chosen that is the standards immediate higher capacity. It is the one that better match the load. The sources and load power dimensioning are summarized in Table 1.

Table 1. Power sources and load dimensioning

Electrical powers	Values	Units
Wind turbine power	300	W
Solar panel power	50	W
Biodiesel generator power	400	W
Battery capacity	200	Ah-24V
DC Load power	300	W
AC Load power	300	W

1.5   PHOTOVOLTAIC (PV) SYSTEM DIMENSIONING AND SIMULATION

1.5.1   PV system design

In this section, the solar energy system is described and designed, and is analyzed in the next section. As mentioned earlier, the solar panel power capacity is 50 W. Based on that, the solar panel model PWX500-12V is chosen. Its characteristics are shown in Table 2. The PV system is designed as shown in Figure 2. It includes solar panel, boost converter,

MPPT controller, battery and resistive load. This load represents all loads connected to DC bus. The PV panel inputs are the solar irradiance and the temperature. Since the solar panel is in the laboratory, the variable lamp light is then used as solar radiation and air conditioning is used for the control of temperature. The lamp light and the air conditioning can be adjusted during experimentations. The working principle of PV system is that the solar panel converts the sun radiation to DC electric power through the photovoltaic cells. Then, the boost converter that consists of an inductor, a switch, a diode and a capacitor is used to increase the solar panel output voltage to match the battery voltage [10]. The MPPT controller aims at controlling the boost converter so that the solar panel can work at maximum power. Several MPPT techniques such as Perturb and Observe, Incremental Conductance, Artificial neural network can be used; students will be learning and testing some of them in the laboratory. The battery is used to store the energy and feed the load if necessary. We note that the boost elements are dimensioned for the PV fixed power of 50 W and the battery voltage of 24 V. For analysis and dimensioning validation purposes, the PV system is simulated with a direct connection to the battery and the load without MPPT.

Table 2. Solar panel characteristics

Parameters	Values	Units
Solar panel power P_{mp}	50	W
Current at maximum power I_{mp}	2.9	A
Voltage at maximum power V_{mp}	17.2	A
Short-circuit current I_{sc}	3.2	A
Open circuit voltage V_{oc}	21.6	V
Nominal cell temperature N_{oct}	25	˚C
Temperature coefficient of I_{sc} (μ_{sc})	1.46×10^{-3}	˚K
Temperature coefficient of V_{oc} (K_d)	-79×10^{-3}	˚K
Cells number N_s	36	

Figure 2. Solar power system

1.5.2   Solar power system simulation

The solar panel module is first modeled and simulated to analyze the I¬V and P¬V characteristics to ensure that the simulations results correspond to the parameters provided by the vendor and to introduce this model in the solar power system model. The I¬V and P¬V output characteristics based on the variation of solar radiation and cells temperature are shown and analyzed according to different scenarios. Figure 3 shows the solar panel output I¬V characteristics at fixed temperature of 25°C and variable sun radiation from 1000 W/m^2 to 200 W/m^2. We observe that when the sun radiation decreases, the solar panel output current and output voltage decrease accordingly. Moreover, this figure shows that I_{sc}=3.2 A and V_{oc}=21.6 V. That corresponds to the value provided by the datasheet. Figure 4 shows the solar panel output I¬V characteristics at fixed sun irradiance of 1000 W/m^2 and variable temperature from 25°C to 100°C. From this figure, we notice that when the temperature decrease, the solar panel output current slightly increases but the voltage decreases largely.

Figure 3. I¬V characteristics with different radiations at 25°C for 50 W PWX500 PV
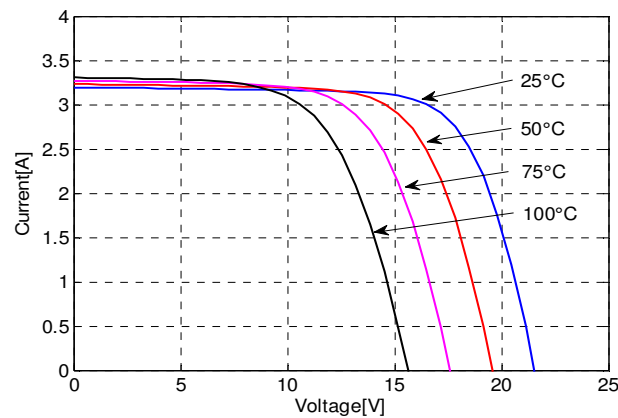
Figure 4. I¬V characteristics with different temperatures at 1000 W/m^2 for 50 W PWX500 PV

Figure 5 shows the solar panel output P¬V characteristics at fixed temperature 25°C and variable sun irradiance from 1000 W/m^2 to 200 W/m^2. We observe from this figure that when the sun irradiance decreases, the solar output power decreases accordingly. Furthermore, we can see that the P¬V output is non-linear curve with a maximum point. Actually, that point corresponds to the Maximum Power Point (MPP) of the solar panel. It can be seen that the MPP is 50 W that is identical to the value given by the datasheet. In order to maintain the solar panel working at that point, a Maximum Power Point Tracking

(MPPT) controller is essential and needs to be implemented [11]. That point is very important as it determines the efficiency of the solar panel. Several MPPT algorithms have been studied in the literature. That includes but not limited to Perturb and Observe (P&O), Incremental Conductance (IC), Fuzzy Logic (FL), Parasitic Capacitance (PC) and Artificial Neural Network (ANN) algorithms [12]. In the laboratory, students will be learning some of these algorithms. Figure 6 shows the solar panel output P¬V characteristics at fixed irradiance of 1000 W/m^2 and variable temperature from 25°C to 100°C. We can see from this figure that when the solar cell temperature increases, the solar output power drops.
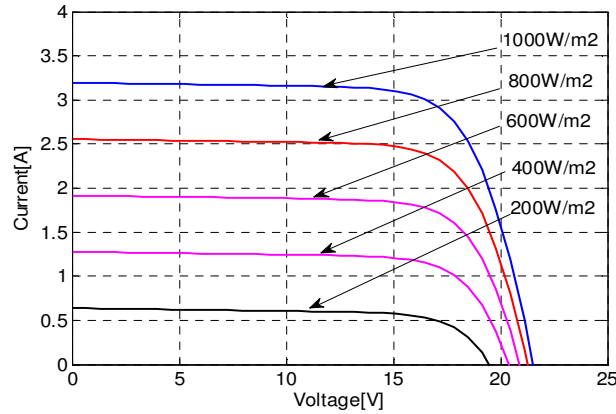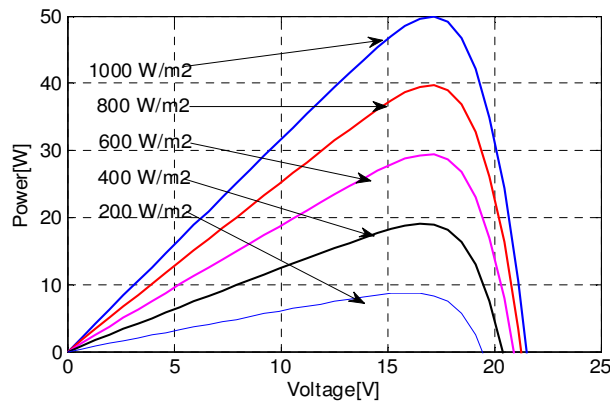

Figure 5. P¬V characteristics with different radiations at 25°C for 50 W PWX500 PV
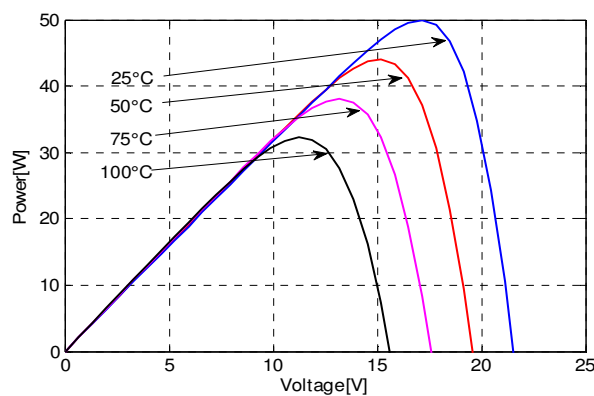
Figure 6. P¬V characteristics with different temperatures at 1000 W/m^2 for 50 W PWX500 PV

After the solar panel tests, the solar power system is connected directly to battery and resistive load and the simulation results are analyzed based on two scenarios:

1) Constant irradiance and variable resistive load

For this simulation, the resistive load is changed from 17 Ω to 5 Ω within 15 s and the solar irradiance is fixed to 1000 W/m^2.

Figure 7 presents the currents evolution of the PV system for variable load where I_{pv} is the solar panel output current, I_{bat} is the battery current and I_{load} is the load current. From this figure, we observe that when the resistive load is high, the PV current is high enough to supply current to the load and charges the battery. However, if the resistive load value decreases, it requires higher current so the PV current is not enough. In this case, the battery discharges by supplying current to the load.
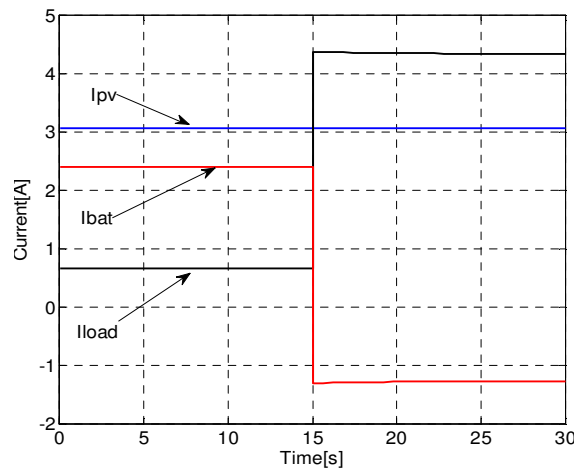
Figure 7. PV, battery and load currents evolution for variable load changing from 17 Ω to 5 Ω at time = 15 s.

2) Variable irradiance and constant resistive load

The solar irradiance varies from 1000 W/m^2 to 200 W/m^2 within 15 s and the resistive load is fixed to 20 Ω. The simulation result is shown in Figure 8. We observe from this

figure that when the solar irradiance is high, the output current I_{pv} is high enough to supply current to the resistive load and charges the battery, but as soon as the irradiance decreases, I_{pv} falls down and the battery starts delivering current to the resistive load. In the laboratory, students will vary the lamp light that represents the solar radiation and the air conditioning that controls the temperature in order to learn the solar system functioning.
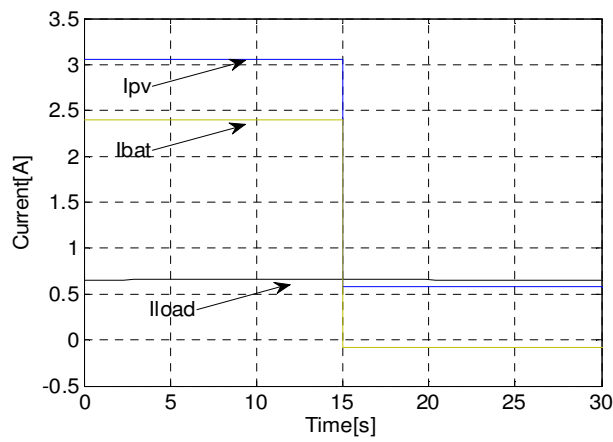
Figure 8. PV, battery and load currents for variable solar irradiance changing from 1000 W/m² to 200 W/m² at time = 15 s

1.6   WECS DIMENSIONING AND SIMULATION

1.6.1   WECS dimensioning

In the proposed HPS, the WECS nominal power is 300 W, so we choose the wind turbine model AIGEOL-300W that can meet ours requirements based on the dimensioning done before. The wind turbine model characteristics are presented in Table 3.

Table 3. Wind turbine characteristics

Parameters	Values	Units
Rotor diameter	2.2	m
Number of blades	3	
Rated output power	300	W
Power max output	450	W
Speed wind minimal start	3	m/s
Rated wind speed	8	m/s
Speed wind operation	3~25	m/s
Security wind speed	40	m/s

The WECS includes wind turbine, permanent magnet synchronous generator (PMSG), rectifier, buck converter, battery and load. The WECS configuration is exhibited in Figure 9.
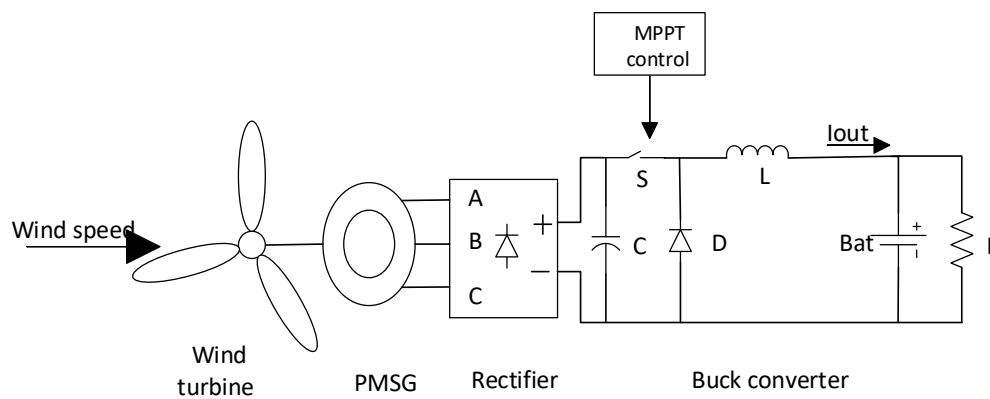
Figure 9. Wind energy conversion system

The only input of the WECS is the wind's speed. Since this system is used in the laboratory, a wind blower is used to provide the wind and vary its speed. The working principle is that the wind turbine converts the wind kinetic energy into DC electrical energy through the PMSG, rectifier and buck converter. The PMSG converts the wind turbine mechanical power to alternative electrical power that is converted by rectifier into DC electrical power. Buck converter is used to adjust the PMSM voltage to the battery voltage and the MPPT controller aims at controlling the buck converter so that the WECS can run at the MPP.

For design purpose, all WECS elements and electronic circuits (rectifier and buck converter) are dimensioned. The dimensioning is based on heavy wind speed conditions (25 m/s). For example, the rectifier diodes' dimensioning is performed by using the following expressions and a safety coefficient where I_{dcR} and V_{dcR} are respectively the wind turbine rectifier output current and voltage:

- Direct average current: $I_{FAV} = I_{dcR}/3$
- RMS current: $I_{FRMS} = I_{dcR}/\sqrt{3}$
- Maximum repetitive reverse voltage (MRRV): $V_{RRM} = \sqrt{3}.\pi.V_{dcR}/\left(3.\sin(\pi/3)\right)$

1.6.2 WECS simulation

The wind turbine model is simulated and analyzed, and the main characteristics are presented. Figure 10 shows the power coefficient $C_p(\lambda,\beta)$ versus the tip speed ratio λ and the pitch angle β. The power coefficient is a non-linear function that represents the efficiency of the wind turbine to convert wind energy into mechanical energy. The tip speed ratio refers to a ratio of the turbine angular speed over the wind speed. The pitch angle refers to the angle in which the turbine blades are aligned with respect to its longitudinal axis [13]. As we can notice from Figure 10, the power coefficient is maximum when the pitch angle $\beta = 0°$.

Figure 11 shows the output power versus the rotor speed and the wind speed. We notice from this figure that at the rated wind speed 8 m/s, the wind turbine power is 300 W that is identical to the rated output power given by the datasheet presented in Table 3.
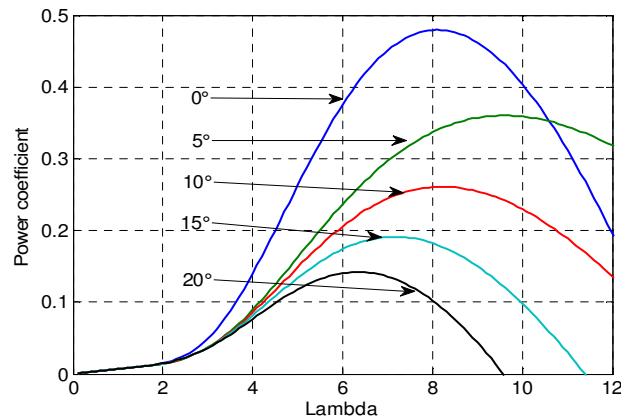
Figure 10. Power coefficient versus the tip speed ratio λ (lambda) and the pitch angle β
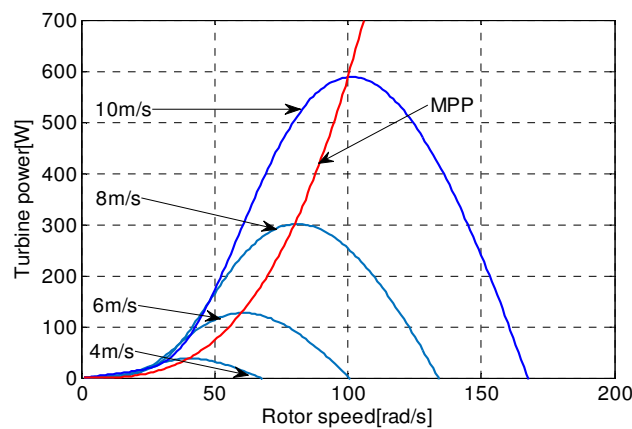
Figure 11. Wind turbine mechanical power versus rotor speed for $\beta =0°$

The turbine mechanical power versus the rotor speed is a non-linear curve with some MPP. Similarly to the solar panel, a MPPT controller needs to be implemented so as to maintain the turbine operation at the MPP. The MPPT algorithms will be taught and learnt

in our laboratory. However, in this paper, we analyze the wind turbine model through a direct connection to battery and resistive load without MPPT. Figure 12 and Figure 13 show respectively the wind turbine mechanical power with constant wind speed and with variable wind speed. We notice that when the wind speed is constant the mechanical power is also constant but when the wind speed varies the mechanical power varies accordingly. Moreover, the WECS currents evolution is analyzed according to two scenarios:
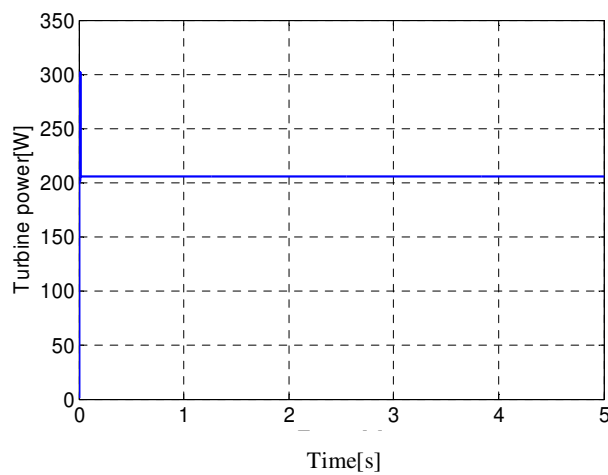
Figure 12. Wind turbine mechanical output power for constant wind speed
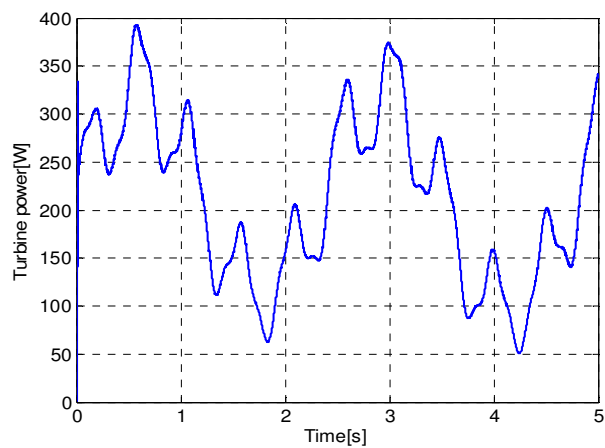
Figure 13. Wind turbine mechanical output power for variable wind speed

1)   Constant wind's speed and variable resistive load

The wind speed is fixed at 8 m/s and the resistive load varies from 30 Ω to 2 Ω. The temperature is fixed to 25 °C. Figure 14 presents the simulation result for this case where I_{wind} is the WECS output current, I_{rload} is the load current and I_{bat} is the battery current. From this figure, we observe that in constant wind speed and variable resistive load scenario, at the step time 2.5 s when the resistive load drops from 30 Ω to 2 Ω, the load current increases, the WECS output current remains constant but the battery current drops down below zero in order to provide the difference. This means the load requires more current but the WECS output current is not enough, so the battery delivers current to the load.

2)   Variable wind speed and constant resistive load

First, the wind speed varies from 8 m/s to 5 m/s and the resistive load is fixed to 5 Ω. The temperature is fixed to 25 °C as well. The simulation result is presented in Figure 15. From this figure, we observe that at the step time 2.5 s when the WECS current drops, the battery current also drops below zero. This means when the wind speed is very low, the WECS output current becomes insufficient, so the battery provides the current to the load. Secondly, the variable wind speed model used is based on the following equation described in [14]. It is a sum of harmonics to display different variation of the wind speed. The resistive load is still fixed to 5 Ω.

$$V = 8 + 0.2\sin(0.1047t) + 2\sin(0.2665t) + 0.2\sin(1.2930t) + 0.2\sin(3.6645t) \qquad (4)$$

The simulation result for this wind speed model is presented in Figure 16. We observe that the battery current profile varies according to the WECS output current profile but the resistive load current is constant. Additionally, we notice that when the WECS output current is lower than the resistive load current, then the battery current drops below

zero to provide the difference. That means the battery provides current to the load at this period.
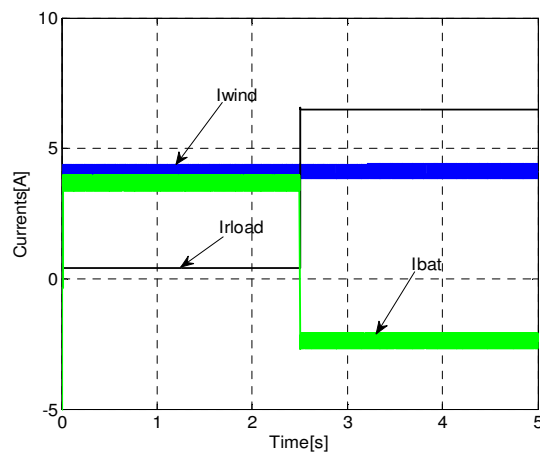
Figure 14. WECS currents evolution for constant wind speed and variable resistive load
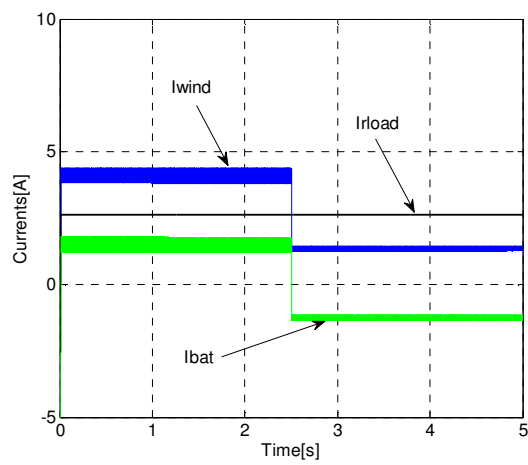
Figure 15. WECS currents evolution for variable wind speed and constant resistive load
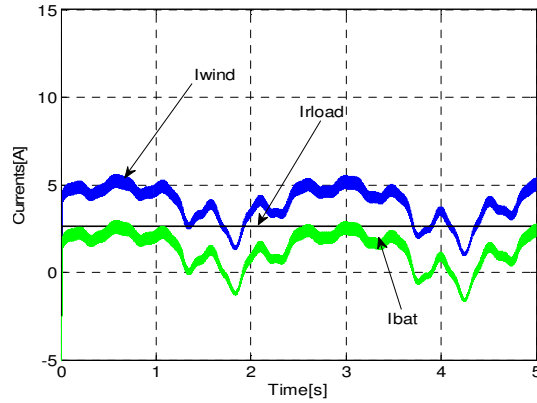
Figure 16. WECS currents evolution for variable wind's speed and constant resistive load

1.7 BIODIESEL GENERATION SYSTEM DIMENSIONING AND SIMULATION

Biodiesel is an alternative diesel fuel made from renewable biological sources such as vegetable oils and animals fats. It is biodegradable and nontoxic and has low emission profiles and so is environmentally beneficial [15]. In the proposed system, biodiesel generator is used as backup to take over the load power supplying. The biodiesel generator system configuration is shown in Figure 17. It includes biodiesel motor, PMSG, rectifier, buck converter, battery, resistive load and DC bus regulation system. The biodiesel motor's speed is regulated at its optimal value. Note that the generation system converters are dimensioned using the same method as for the WECS. V_{ref} is the voltage which allows the battery charging and it is chosen slightly higher than the DC bus battery voltage.

The biodiesel generation system is simulated and the simulation output results are depicted below in Figure 18 and Figure 19 where I_{gen} is the generation system output current, I_{bat} is the battery current, I_{rload} is the resistive load current and V_{dc} is the DC bus voltage. In this simulation, the load value is changed from 40 Ω to 20 Ω at step time 2.5 s. From Figure 18, we observe that when the load current increases, then the battery current decreases by the same value, but the generation system current keeps the same. The

meaning of this is that, when the load requires more current, then the generator decreases the battery charging current so as to satisfy the load requirements. But in Figure 19, we notice that the DC bus voltage is maintained despite the load variation. That is due to the fact that the DC bus voltage is regulated.
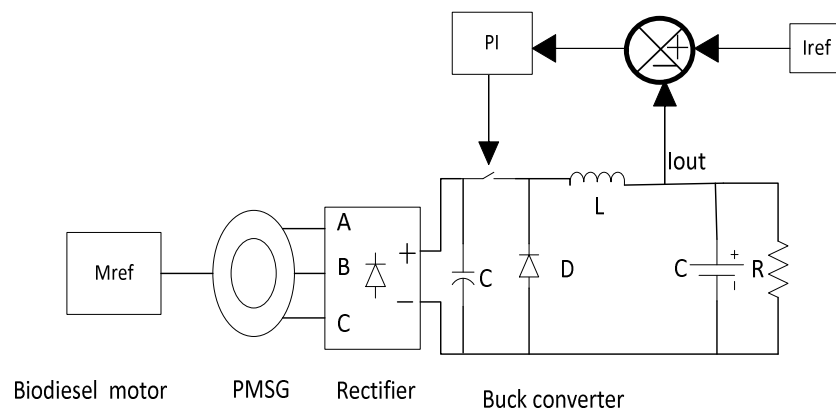
Figure 17. Biodiesel generator system
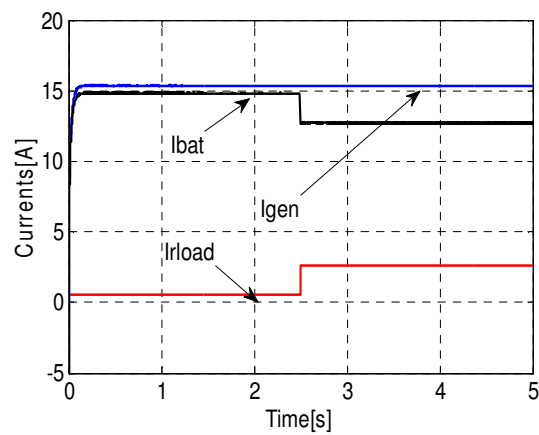
Figure 18. Generator, battery and load currents showing Ibat decreases at 2.5 s when Irload increases
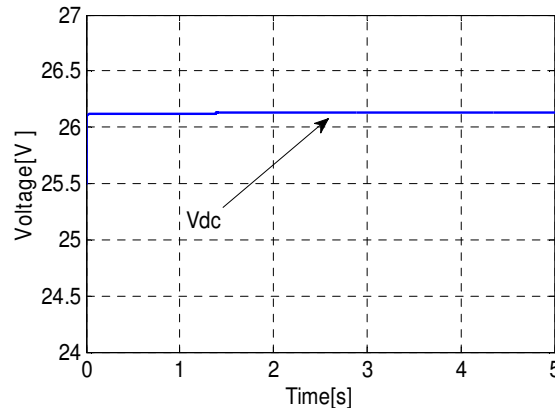
Figure 19. Output voltage of DC-DC converter maintained constant

1.8 HPS SIMULATION AND RESULTS

The WECS, the PV system and the BDG are coupled and integrated in the same simulation environment in order to evaluate the hybrid power system behavior under variations of input parameters. This system is simulated and analyzed according to two cases which are developed below. As reminder, the PV panel rated power is 50 W, the wind turbine is 300 W, the BDG is 400 W and the load maximum power consumption is 300 W.

1) **First case**: The BDG doesn't work all the time, the wind turbine works at the rated power for half time and stop for the rest of the time, the PV keeps working at its rated power all the time. We observe in Figure 20-a that the PV power delivered is around the rated power 50 W all the time whereas the WECS power delivered is around 300 W within half time and then drops down to zero for the rest of the time. Consequently, the PV and WECS total power drops down after half time as shown in Figure 20-c. The Figure 20-e shows that the battery current drops below zero, which means the battery discharged by supplying current to the load. This result show that the hybrid power system was capable of providing necessary power to the load despite the low wind speed as shown in Figure 20-d. Actually, during the first half time, the WECS and the PV deliver the power to the load and

store the rest in the battery so in the second half time, it was able to feed the load when the WECS stopped.
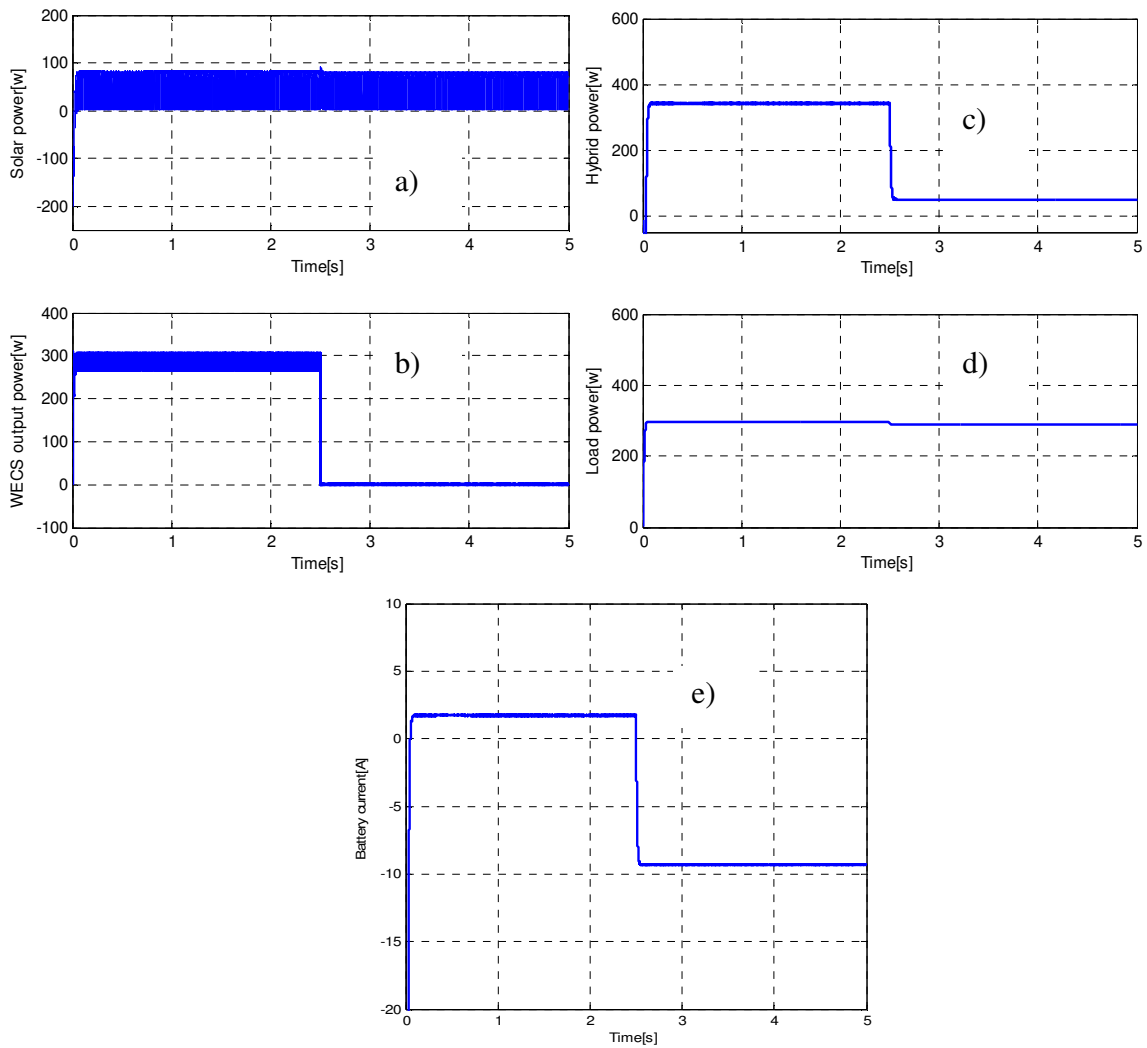
Figure 20. Hybrid system response during the first case: (a) PV power; (b) WECS power; (c) hybrid power; (d) load power and (e) battery current

1) **Second case**: The BDG works in the first half time and stops working for the rest of time, the wind turbine starts working at the rated power during the second half time and the PV doesn't work all the time. We observe in Figure 21-a that the BDG power delivered is 400 W in the first half time and drops down to zero for the rest of the time, and the Figure 21-b shows that the WECS delivered power is around 300 W during the second half time. Consequently, the BDG and WECS total power delivered is around 400 W for the first half time and 300 W for the second half time as presented in Figure 21-c. The Figure 21-e shows that in the first half time, the battery current is above zero around 3.5 A and in the second half it is below zero around -0.15 A. That means that the battery was charged during the first half time and discharging in the second half time. Actually, during the first half time, the BDG delivers the power to the load and charges the battery. In the second half when the BDG stops, only the WECS supplies the power to the load, but the power is not enough, so the battery discharging by delivering power to the load.
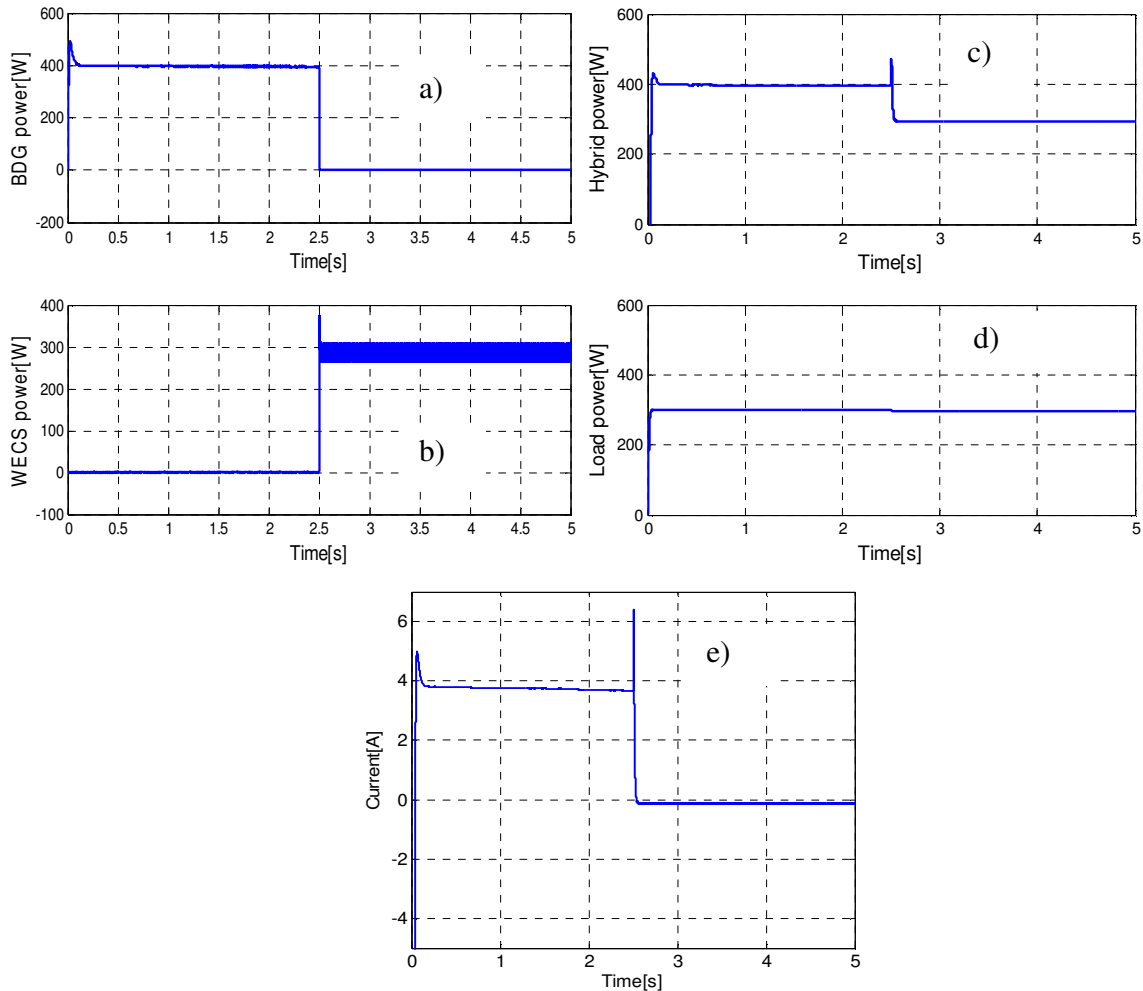
Figure 21. Hybrid system response during the second case: (a) BDG power; (b) WECS power; (c) hybrid power; (d) load power and (e) battery current

1.9 LABORATORY ENVIRONMENT

1.9.1 Physical environment

The physical environment of the renewable energy laboratory is shown below in Figure 22. It includes wind blower, wind turbine, solar panels, insolation system, biodiesel

generator, coupling units, batteries, and usual laboratory equipment's. Information and Communication Technology (ICT) units are also included. The whole system unit is instrumented and using real time acquisition systems: the speed of the fan, the wind speed at the end of the blower, the temperature of the air, the rotation speed of the turbine, the insolation, the power output of all units, the signals (currents and voltages) at the ends of each electrical unit as well as the temperature of the batteries are all monitored. All data are acquired using DAQ LabVIEW unit.
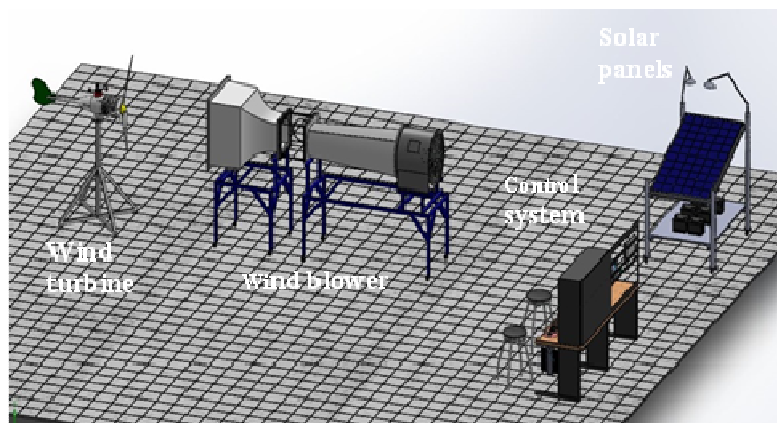
Figure 22. Physical architecture of the renewable energy laboratory

1.9.2   Virtual platform

The purpose of the laboratory is to allow on-site learning and e-learning via a virtual platform. In that end, the laboratory will be physically implemented at the Université du Québec à Rimouski. Engineer students in renewable energy field can learn all aspects of renewable energies and take hands-on all materials to deepen their knowledge. In addition to on-site students in the laboratory, students can remotely access to the laboratory via the virtual platform and the e-learning system upon granted permissions by laboratory supervisors. Via the virtual platform, shown in Figure 23, students can interact with each other's in 'people-to-people' way or interact with materials in 'people-to-equipment' way

either in real-time (synchronous) mode or off-line (asynchronous) mode. In the laboratory, a monitoring application will be developed with LabVIEW software to monitor the whole system and to measure the different signals through web use interface.

The laboratory will be equipped with computers, large videoconference screen, webcam, microphone, speakers and internet connection. Remote students can collaborate with the laboratory students via the videoconference system. Furthermore, remote students will be able to interact with the laboratory equipment via a Virtual Private Network (VPN) implemented between all sites Local Area Network (LAN) using high speed internet connection. IP cameras will be positioned adequately to visualize the whole laboratory. Remote student's credentials will be reviewed before granting any permission to access the system.
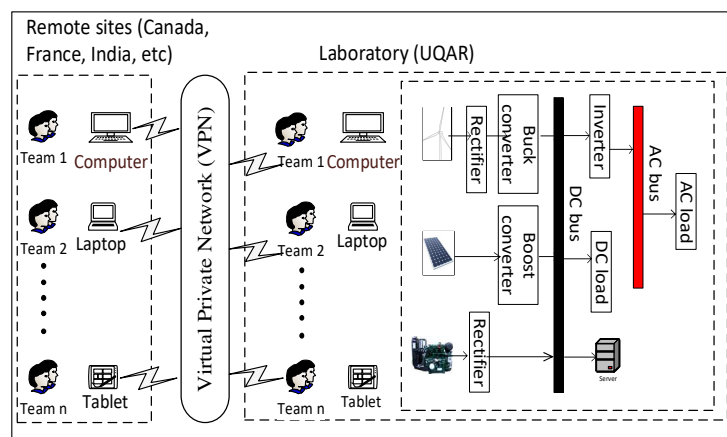
Figure 23. Virtual platform architecture

1.9.3 E-Learning

E-learning is having a great impact on education nowadays. It consists of the integration of Information and Communication Technology (ICT) in education system; and then enable the use of new multimedia technologies of the internet in improving learning

quality in remote collaboration mode [16]. The big advantage of e-learning is to allow students who don't have access to renewable energy laboratory in their university to interact with others students to share knowledge and take hands-on materials that they don't have in their university. This will be a good way to promote renewable energy to students all over the world. E-learning is becoming more and more cost effective teaching and learning solution in the world. Actually, it enables to share laboratory between different educational institutions and organizations and overcome distance challenges.

In the e-learning system, several courses and students assessments will be available online for students to learn different aspects of renewable energies such as: renewable energy production and optimization, power flow determination, limit of Betz, solar radiation effects, efficiency, renewable energy systems control, MPPT, etc. The following courses will taught in the laboratory in terms of experiments: renewable energies, wind energy, power electronics, fluid mechanic, etc.

1.10 Conclusion

A new renewable energy laboratory concept based on the integration of wind, solar and biodiesel energies sources was presented. The hybrid power system, the laboratory physical environment, the laboratory virtual platform and the e-learning concept were exhibited. The solar power system, the wind power system and the biodiesel generator working principle and their dimensioning and simulation were shown. The simulation results indicates that both the solar panel and wind turbine are non-linear system and MPPT controller needs to be implemented to maintain them working at the maximum power point so as to increase their efficiency. Moreover, the solar system and WECS currents evolution show that the battery is of vital importance in renewable energy system because it can store energy in high production period of renewable sources and feed the load in low production period. The e-learning concept was also addressed in this paper which displays the new

trend of learning. The three renewable energy sources coupling strategy and the MPPT controllers will be developed in future paper.

1.11 REFERENCES

[1]   S. Kumar and V. K. Garg, "A hybrid model of solar-wind power generation system," International Journal of Advanced Research in Electrical, Electronics and Instrumentation Engineering, vol 2, pp. 4107-4016, 2013.

[2]   O. C. Onar, M. Uzunoglu, and M. S. Alam, "Dynamic modeling, design and simulation of a wind/fuel cell/ultra-capacitor-based hybrid power generation system," Journal of Power Sources, vol. 161, pp. 707–722, 2006.

[3]   O. A. Herrera and D. A. Fuller, "Collaborative model for remote experimentation laboratories used by non-hierarchical distributed groups of engineering students," Australasian Journal of Educational Technology, vol. 27, pp. 428-445, 2011.

[4]   K. Bauer and L. Mendes, "WebLab of a DC motor speed control didactical experiment," Campus-Wide Information Systems, vol. 29, pp. 281-290, 2012.

[5]   I. Calvo, M. Marcos, D. Orive, and I. Sarachaga, "Building complex remote learning laboratories," Computer Applications in Engineering Education, vol. 18, pp. 53-66, 2010.

[6]   C. A. Jara, F. A. Candelas, F. Torres, S. Dormido, and F. Esquembre, "Synchronous collaboration of virtual and remote laboratories," computer applications in engineering education, vol. 20, pp. 124-136, 2012.

[7]   E. Fabregas, G. Farias, S. Dormido-Canto, S. Dormido, and F. Esquembre, "Developing a remote laboratory for engineering education," Computers and Education, vol. 57, pp. 1686-1697, 2011.

[8]   M. Abdulwahed and Z. K. Nagy, "Developing the triLab, a triple access mode (hands-on, virtual, remote) laboratory, of a process control rig using LabVIEW and Joomla," Computer Applications in Engineering Education, vol. 21, pp. 614-626, 2013.

[9]   S. K. Ramoji, B. B. Rath, and D. V. Kumar, "Optimization of hybrid PV/wind energy system using genetic algorithm (GA)," Journal of Engineering Research and Applications, vol. 4, pp. 29-37, 2014.

[10]   S. Alsadi and B. Alsayid, "Maximum Power Point Tracking Simulation for Photovoltaic Systems Using Perturb and Observe Algorithm," International Journal of Engineering and Innovative Technology, vol. 2, pp. 80-85, 2012.

[11]   J. A. Jiang, T. L. Huang, Y. T. Hsiao and C. H. Chen, "Maximum power tracking for photovoltaic power systems," Tamkang Journal of Science and Engineering, vol. 8, pp. 147-153, 2005.

[12] R. Ramaprabha, B. L. Mathur, and M. Sharanya, "Solar array modeling and simulation of MPPT using neural network," Conference on Control, Automation, Communication and Energy Conservation, 2009.

[13] M. Chandramouly, B. B. Naik, and M. T. Naik, "Hybrid wind-solar energy system with rectifier technology," International Journal of Advanced and Innovative Research, vol. 2, pp. 686-694, 2013.

[14] A. Mirecki, Etude Comparative de Chaînes de Conversion d'Énergie Dédiées à une Éolienne de Petite Puissance, Thesis, Institut National Polytechnique de Toulouse, France, 2005.

[15] F. Maa and M. A. Hanna, "Biodiesel production: a review," Bioresource Technology, vol. 70, pp. 1-15, 1999.

[16] C. A. Jara, F. A. Candelas, F. Torres, S. Dormido, F. Esquembre, and O. Reinoso, "Real-time collaboration of virtual laboratories through the Internet," Computers and Education, vol. 52, pp. 126-140, 2009.

CHAPITRE 2
MODELISATION ET SIMULATION D'UN SYSTÈME D'ÉNERGIE HYBRIDE BASÉ SUR L'INTÉGRATION DE L'ÉNERGIE ÉOLIENNE, SOLAIRE ET DU BIODIESEL AINSI QU'UNE BATTERIE DE STOCKAGE

2.1 RESUME EN FRANÇAIS DU DEUXIEME ARTICLE

Cet article présente la modélisation, la simulation et le contrôle d'un système d'énergie hybride intégrant un système de conversion d'énergie éolienne, un système solaire photovoltaïque et une génératrice au biodiesel en incluant une batterie de stockage. Ce système hybride est conçu pour assurer la fiabilité énergétique sous toutes les conditions météorologiques. Le modèle de ce système comprend une éolienne, des panneaux solaires photovoltaïques, une génératrice synchrone à aimants permanents, des convertisseurs de puissance (hacheurs et redresseurs) et des contrôleurs de suivi du point de puissance maximale (MPPT). L'algorithme de contrôle MPPT Perturber et Observer (P&O) est utilisé pour extraire le maximum de puissance des panneaux photovoltaïques et la technique (TSR) est utilisée pour extraire le maximum de puissance de la turbine éolienne. Le fonctionnement du système hybride proposé est examiné sous différentes conditions en fonction de la variation de la vitesse du vent et des radiations solaires. La génératrice au biodiesel est utilisée uniquement comme une source d'énergie de secours lorsque l'état de charge de la batterie (SOC) est inférieur à 45%. Une technique d'hystérésis est utilisée pour commander la mise en marche de la génératrice en fonction de la variation de l'état de charge de la batterie. Le système développé est constitué d'un panneau photovoltaïque de 50 W, une éolienne de 300 W, une génératrice au biodiesel de 400 W et une batterie de 24

V et de 200 Ah. Le modèle proposé démontre une bonne stratégie pour assurer la fiabilité de puissance dans toutes les conditions en utilisant les énergies renouvelables.

Le but du deuxième article était d'étudier de façon détaillée le fonctionnement et le contrôle des différentes sources d'énergie à savoir le système solaire, éolien et celui de la génératrice au biodiesel. De plus, l'étude du couplage des différentes sources via des scénarios suivant les variations de vitesse du vent et des radiations solaires a été élaborée. Les techniques de poursuite du point de fonctionnement optimal Tip Speed Ratio (TSR) et Perturber et Observer (P&O) ont été appliqués respectivement au système éolien puis au système solaire afin d'extraire le maximum de puissance possible. Les sources ont été modélisées et simulées avec le logiciel Matlab/Simulink.

Ce deuxième article intitulé « Modeling and Simulation of Hybrid Power System Integrating Wind, Solar, Biodiesel Energies and Storage Battery » fut rédigé par moi-même. En tant que premier auteur, ma contribution à ce travail fut l'essentiel de la recherche sur l'état de l'art, le développement de la méthode et la rédaction de l'article. Le professeur Ahmed Chebak, second auteur, a fourni l'idée originale. Il a aidé à la recherche sur l'état de l'art, au développement de la méthode ainsi qu'à la révision de l'article. Les professeurs Abderazak El Ouafi et Mustapha Mabrouki ont contribué avec leurs commentaires sur la méthodologie adoptée et ont participé à la révision de l'article. Cet article a été soumis et accepté à la conférence « IEEE International Renewable and Sustainable Energy Conference » à Marrakech (Maroc) en Novembre 2016.

2.2   MODELING AND SIMULATION OF HYBRID POWER SYSTEM INTEGRATING WIND, SOLAR, BIODIESEL ENERGIES AND STORAGE BATTERY

ABSTRACT

This paper presents the modeling, simulation and control strategy of a hybrid power system (HPS) integrating a wind energy conversion system (WECS), a solar photovoltaic system (SPV) and a biodiesel generator (BDG) as well as a storage battery designed to ensure power reliability under all various weather conditions. The model includes wind turbine, photovoltaic panels, permanent magnet synchronous generator (PMSG), power converters and maximum power point tracking (MPPT) controllers. Perturb and Observe (P&O) algorithm is used to extract the maximum power from PV and Tip Speed Ratio (TSR) controller for the WECS. The dynamic behavior of the proposed HPS is examined under different conditions based on wind speed variation and solar radiations. The BDG is involved only for backup when the battery state of charge (SOC) is less than 45%. A hysteresis technique is used to control the BDG start-up based on the variation of the battery SOC. The developed HPS consists of a 50 W photovoltaic panel, 300 W wind turbine, 400 W biodiesel generator and 200 Ah/24 V battery. The resultant model offers a good strategy to ensure power reliability under all conditions using renewable energies.

Keywords—hybrid power system; control strategy; modeling; simulation; maximum power point tracking; renewable energy.

2.3   INTRODUCTION

The fight against the global climate warming is getting fiercer since last decade. Renewable energies have been found as a key promising alternative solution to fossil fuels which are largely responsible for that issue. Among the renewable energies, wind and solar

power developments are the ones that are known for an impressive rapid growth in the industry. However, both solar and wind energy systems are facing efficiency problems. For several years, researchers have been investigating techniques to increase their efficiency. Actually, the solar and wind energies depend respectively on solar radiation and wind speed that are really difficult to predict and vary greatly from season to another which certainly affects their efficiency and reliability. Moreover, both wind and solar systems are non-linear systems with a maximum point called maximum power point (MPP). To reach this MPP, a maximum power point tracking (MPPT) controller should be applied [1-3]. Many techniques were proposed and published in the literature. These techniques include but not limited to: increment conductance, constant voltage method, constant current method, curve-fitting, steepest descent, perturb and observe (P&O), fuzzy logic (FL), artificial neural network (ANN). The selection between these methods is based on the cost, the complexity, the accuracy, the convergence speed and the applicability [4]. The method used in this paper for the solar power is the P&O technique which is one of the most used MPPT algorithms, because of its easy implementation [5, 6]. For the wind energy system, Tip Speed Ratio (TSR) control method is adopted because of its good performance with fast response and high efficiency [7].

To ensure power reliability, many scientists recommend to not use one intermittent power source such as solar or wind but suggest the integration of both of them working either together or alternatively. That is named hybrid power system. Many investigations have been conducted in hybrid power system. M. Natsheh and A. Albarbar [8] proposed an hybrid power system based on wind and solar energy using storage battery. S. Kumar and V. K. Garg [9] presented a hybrid solar-wind system with storage fuel cell in India. C. Marisarla and K. R. Kumar [10] introduced a hybrid wind and solar energy system with battery storage for an isolated system. However, these solutions can't fully ensure continuous power supply since the wind speed and sunshine are unpredictable and the battery energy can sometimes be insufficient.

This paper proposes a hybrid power system which consists in the integration of three renewable energy sources composed of wind, solar and biodiesel energies as well as a storage battery in order to increase the power stability and reliability. The biodiesel generator is used as backup and works only when the wind and solar energy doesn't meet the load requirement and the storage battery energy is low. A hysteresis technique is used to control the BDG start-up. This system can work under all weather conditions despite the solar irradiance and wind speed variation. The solar power, the wind energy and the biodiesel generator systems are then modeled, simulated and analysed using Matlab/Simulink Software. The adopted hybrid power system is first presented. Afterwards, the control strategy is performed. Finally, simulations results are presented and discussed.

2.4   HYBRID POWER SYSTEM

The proposed hybrid power system consists of PV panels, wind turbine, biodiesel generator, storage battery, DC-DC and AC-DC converters, and DC load. The schematic representation of the system is shown in Figure 24 and the electrical rated powers of all components are as follow: the wind turbine is 300 W, the solar panel is 50 W, the biodiesel generator is 400 W, the battery capacity is 200 Ah-24 V and the DC load is 300 W.
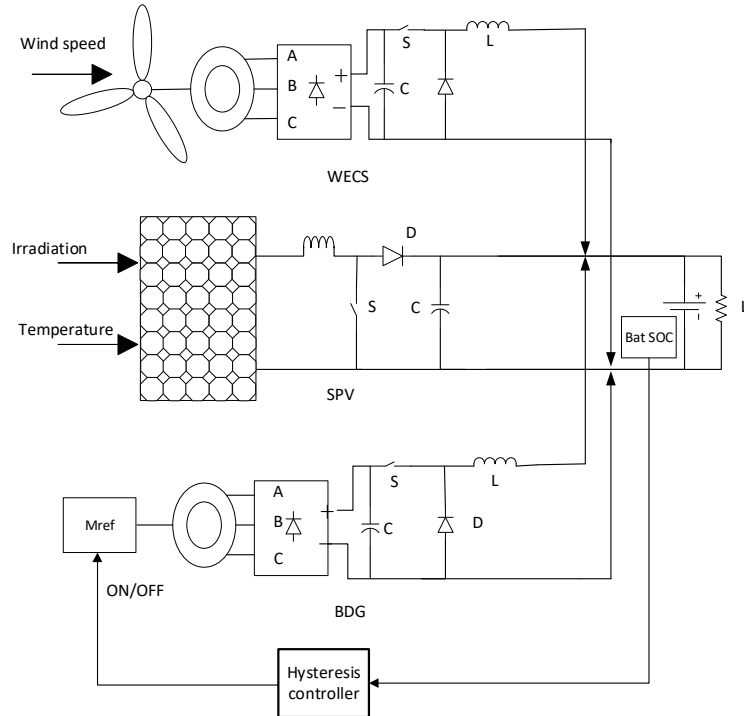
Figure 24. Proposed hybrid power system

2.5 SOLAR PHOTOVOLTAIC SYSTEM

2.5.1 Modeling and design of PV module

Solar module is composed of several cells mounted in series and/or in parallels. When mounted in series, the total voltage is the sum of every cell voltage and the current keeps the same. On the opposite, when mounted in parallels, the current is the sum of every cell current and the voltage keeps the same. Our solar module includes 36 cells mounted in series. The considered equivalent circuit of solar cell is depicted in Figure 25. It consists of photocurrent, diode, shunt resistor and series resistor. The used mathematical model of the solar cell is based on the photovoltaic current equation as follow

$$I_{pv} = I_{ph} - I_s (\exp \frac{q(V + R_s I)}{AKT} - 1) - \frac{V + R_s I}{R_{sh}} \qquad (5)$$

where I_{ph} is the photonic current, I_s is the saturation current dependent on cell temperature, q is the electric charge (1.6×10^{-19} Coulombs), K is Boltzmann's constant (1.38×10^{-23} J/K), T is the cell's absolute temperature, A is the idealizing factor, R_s is the series resistance, R_{sh} is the shunt resistance, V is the cell output voltage. The photocurrent I_{ph} mainly depends on solar radiation and cell temperature as seen in the following equation

$$I_{ph} = (I_{sc} + K_i(T - 298)) \frac{G}{1000} \qquad (6)$$

where I_{sc} is the short-circuit current, K_i is the current coefficient temperature, G is the current irradiance in (W/m^2) and 1000 is the irradiance at standard operating conditions. Furthermore I_s is the cell's reverse saturation current specified as below [11]

$$I_s = \frac{I_{sc} + K_i \Delta T}{\exp(\frac{V_{oc} + K_v \Delta T}{AV_t}) - 1} \qquad (7)$$

where V_{oc} is the voltage open circuit, K_v is the voltage coefficient temperature, ΔT is the temperature at standard operating conditions and $V_t = N.K.T / q$ where N is cells number.
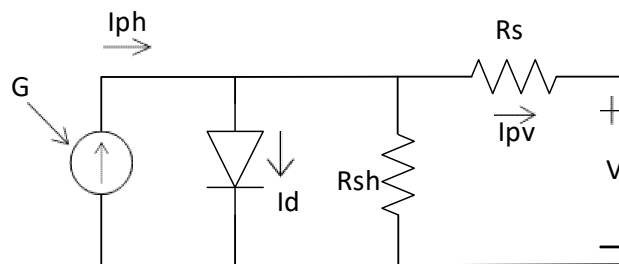
Figure 25. Solar cell equivalent circuit

2.5.2 Solar photovoltaic control system

The proposed PV model is PWX500 and its specifications are shown in Table 4.

Table 4. Solar panel characteristics

Parameters	Values	Units
Solar panel power P_{mp}	50	W
Current at maximum power I_{mp}	2.9	A
Voltage at maximum power V_{mp}	17.2	A
Short-circuit current I_{sc}	3.2	A
Open circuit voltage V_{oc}	21.6	V
Nominal cell temperature N_{oct}	25	˚C
Temperature coefficient of I_{sc} (μ_{sc})	1.46×10^{-3}	˚K
Temperature coefficient of V_{oc} (K_d)	-79×10^{-3}	˚K
Cells number N_s	36	

The PV system is a non-linear system with a MPP. In order to maintain the system working at the MPP, a boost converter is inserted between the PV and the load. The P&O algorithm is adopted to tune the duty cycle of the boost converter to keep the PV system at the maximum point. The working principle of this algorithm is that a slight perturbation is introduced to the system which changes the module power. If the power increases due to the perturbation, then the perturbation is continued in that direction. After the peak power is reached, the power at the next step decreases and hence after that the perturbation reverses. When the steady state is reached, the algorithm oscillates around the peak point [11]. The P&O algorithm flow chart is shown in Figure 26 where P is the SPV output power, V the output voltage and D the duty ratio of the converter. The adopted SPV system is presented in Figure 27.
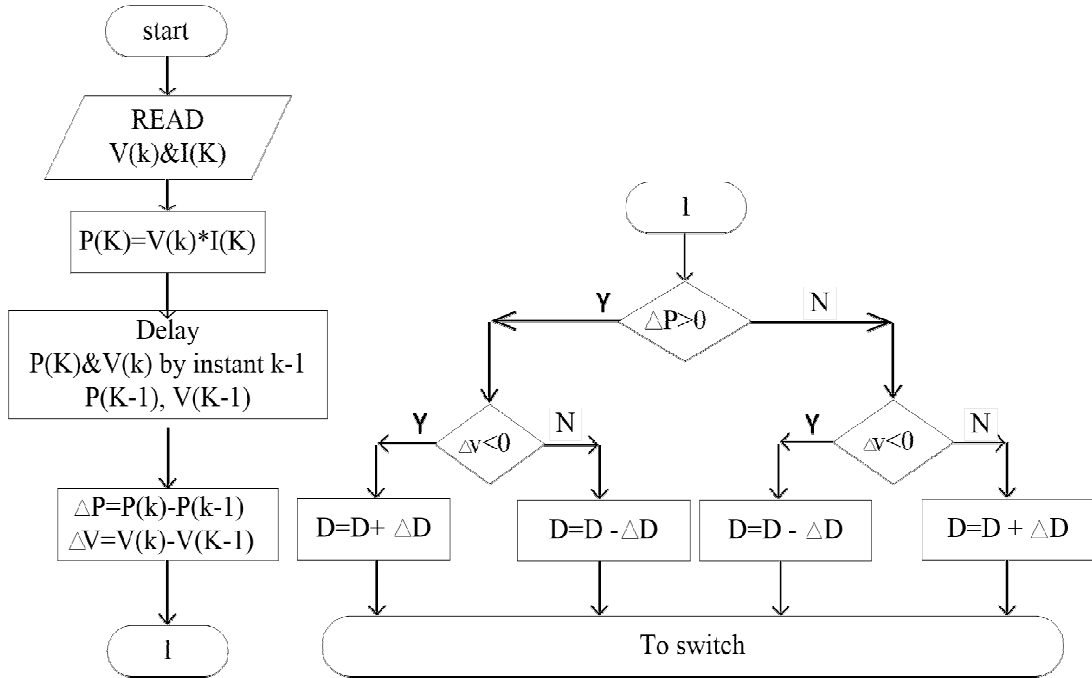
Figure 26. Perturb and Observe algorithm flow chart
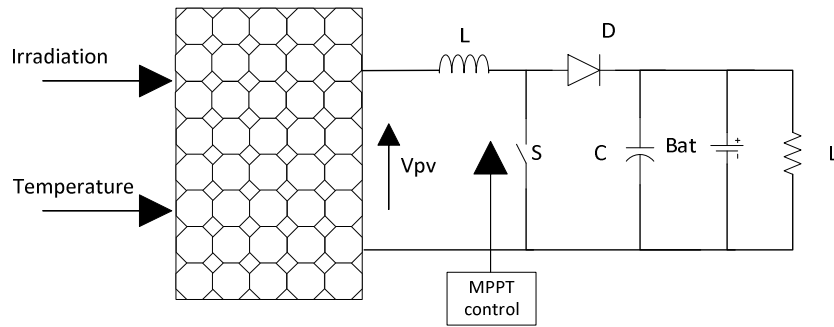
Figure 27. Solar photovoltaic power system

The power flow of the DC-DC converter is controlled by varying the ON/OFF duty cycle of the converter. The average output voltage is determined by the equation

$$\frac{V_{out}}{V_{in}} = \frac{1}{1-D} \qquad (8)$$

where D is the duty cycle, V_{out} is the DC-DC converter output voltage and $V_{in} = (V_{in} = V_{pv})$ is the input voltage. The SPV system is simulated with a variable solar irradiance and the results are presented below. Figure 28-a displays the solar irradiance profile and in Figure 28-b it is shown that the boost converter output power oscillate around the input boost converter (P_{in}). In Figure 28-c, it is proved that the SPV works around the reference voltage (17.2 V) between 4 and 6 seconds which correspond to its maximum power point.
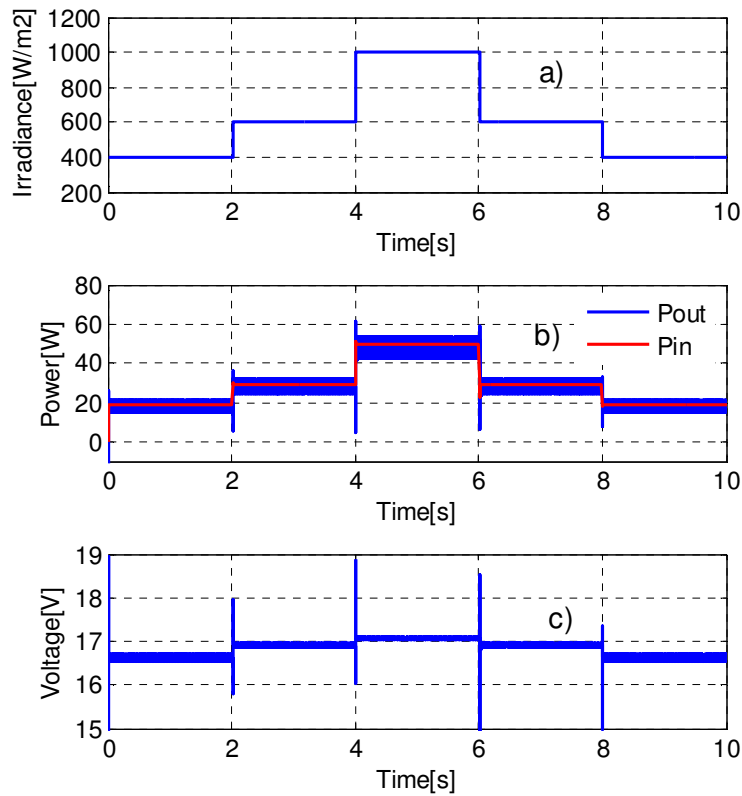
Figure 28. PV system with variable irradiance: a) solar irradiance profile, b) output and input power and c) reference voltage

Figure 29 clearly demonstrates that the SPV output power oscillates around its maximum power for each irradiance. The irradiances applied are 200 W/m^2, 400 W/m^2, 600 W/m^2, 800 W/m^2 and 1000 W/m^2. The oscillation is illustrated by a cloud of points for each irradiance around the MPP respectively. The peak is reached at 1000 W/m^2 with power oscillation around 50 W.
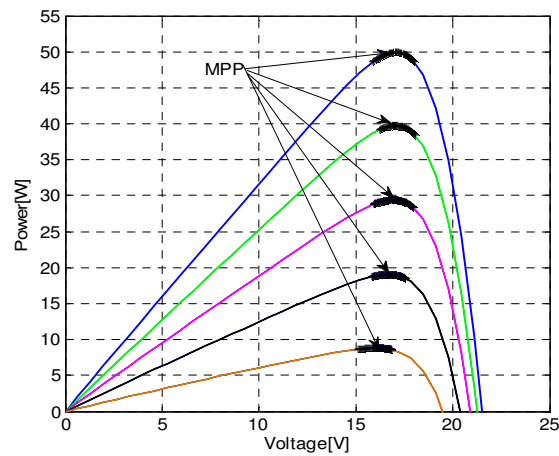
Figure 29. Maximum power points with irradiance variation with the P&O algorithm.

2.6   WIND ENERGY CONVERSION SYSTEM

2.6.1   Modeling and design of WECS

The wind energy conversion system is presented in Figure 30 and the wind turbine characteristics in Table 5. The WECS converts the wind kinetic energy into electrical energy. The actual mechanical power provided by wind turbine is given by the equation

$$P_w = \frac{1}{2}\rho C_p(\lambda, \beta)AV^3 \tag{9}$$

where ρ is the air density, A is the swept area of the rotor blade, it is equal to πR^2, v is the wind speed, and $C_p(\lambda, \beta)$ is the power coefficient. The power coefficient determines the efficiency of the wind turbine depending on the Tip Speed Ratio (λ) and the pitch angle (β). Parameter λ stands for the ratio between turbine speed and the wind speed. It is given by the equation

$$\lambda = \frac{\omega R}{v} \tag{10}$$

where ω is the turbine angular speed, R is the turbine blade radius. The power coefficient $C_p(\lambda, \beta)$ depends on the wind turbine characteristics. The model used in this paper is the one described in [12] by the equation

$$C_p(\lambda,\beta) = 0.5176(\frac{116}{\lambda} - 0.4\beta - 5)e^{-\frac{21}{\lambda}} + 0.0068\lambda \tag{11}$$

where

$$\frac{1}{\lambda} = \frac{1}{\lambda + 0.08\beta} - \frac{0.035}{1 + \beta^3} \tag{12}$$

Theoretically, the wind turbine maximum power coefficient is 0.59 which is called the limit of Betz, but the practical range is between 0.2 and 0.4 [13].
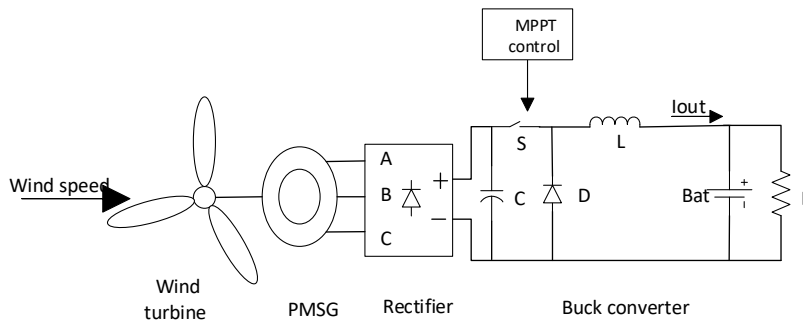
Figure 30. Wind energy conversion system

Table 5. Wind turbine characteristics

Parameters	Values	Units
Rotor diameter	2.2	m
Number of blades	3	
Rated output power	300	W
Power max output	450	W
Speed wind minimal start	3	m/s
Rated wind speed	8	m/s
Speed wind operation	3~25	m/s
Security wind speed	40	m/s

2.6.2 WECS control system

The wind turbine is a non-linear system; therefore it does not always work in optimal condition. In order to keep it working at maximum condition, a MPPT controller is used. In this paper, the tip speed ratio (TSR) technique is adopted. The process to get the maximum power of the wind turbine goes as follow.

The optimum power of the wind turbine is given by the following equation considering the optimal tip speed ratio λ^{opt} and $\beta = 0$.

$$P_{eol}{}^{opt} = \frac{1}{2}\rho C_p(\lambda^{opt})AV^3 \tag{13}$$

Taking into account the WECS efficiency η, the output optimum power is calculated as below

$$P_{out}^{opt} = U_{out} I_{out}^{ref} = \eta P_{eol}^{opt} \tag{14}$$

where I_{out}^{ref} is the output reference current. From equation (14), the reference current is obtained by

$$I_{out}^{ref} = \frac{\eta P_{eol}^{opt}}{U_{out}} \tag{15}$$

To maximize the output power, we need to control the output current that is the inductor current for which voltage is given by

$$U_L(t) = L\frac{dI_{out}}{dt} \tag{16}$$

From this equation, we obtain the output current equation

$$I_{out}(p) = \frac{1}{L.p}U_L \tag{17}$$

A PI controller is used to regulate this output current. The regulation method is illustrated in the Figure 31. To get the PI controller parameters, the following closed-loop transfer function is used. The values are K_p=27.2, K_i=49348, T_i=0.551ms and L=10 mH.

$$G(p) = (K_p + \frac{K_i}{p})\frac{1}{L.p} = \frac{K_i}{L}\frac{pT_i+1}{P^2} \tag{18}$$
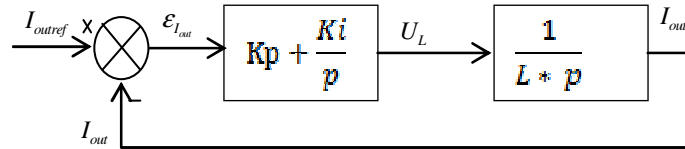
Figure 31. WECS closed-loop control system

The WECS output power is analyzed with a variable input wind speed. Figure 32-a displays the wind speed profile and in Figure 32-b it is shown that the extracted mechanical output power (WTP) follow very well the optimal power (P_{opt}), which means that the TSR control system was able to maintain the WECS working at its optimal condition. Furthermore, in Figure 32-c, we can see that the obtained power coefficient (C_P-TSR) is around the optimal one (C_P-max) which is 0.48. In addition, Figure 32-d proves that the output current (I_{out}) follows the input reference current (I_{ref}) in order to extract the maximum power from the wind turbine.
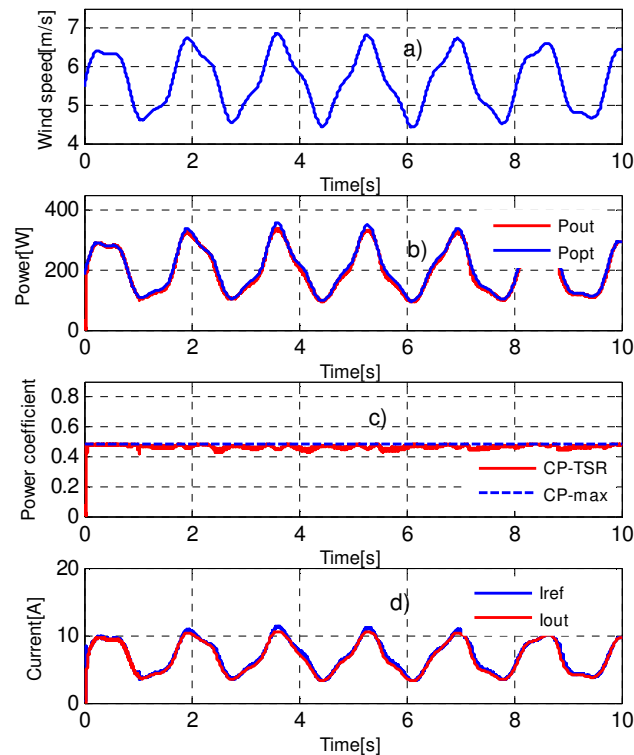
Figure 32. a) Wind speed profile, comparison b) between WT mechanical power and the optimal power, c) between maximum power coefficient and the obtained power coefficient, and d) between the reference current and the output current

2.7 BIODIESEL GENERATOR

As an important alternative to diesel fuel, biodiesel is considered sustainable and environmentally friendly and has attracted increased interest over the last few decades. It is typically defined as a mixture of fatty acid alkyl esters obtained from a process known as transesterification, in which triglycerides from vegetable oils, animal fats, and even waste cooking oils react with alcohol in the presence of a catalyst [14-16]. In the proposed system, a generator fueled with biodiesel is used as backup to take over the load power supplying when the PV and WECS are not sufficient and the battery state of charge (SOC) has dropped. The biodiesel generator system configuration is shown in Figure 33. It includes biodiesel motor, PMSG, rectifier, buck converter, battery, resistive load and output current regulation system. The biodiesel output current is regulated with the rated output current taken as reference current. Figure 34 shows the BDG output power obtained from the simulation. We can see that the BDG is able to provide the rated output power for 20 Ω constant load.
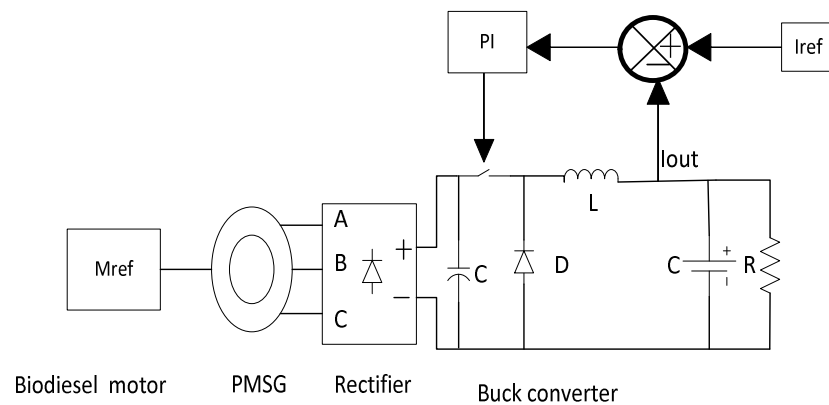
Figure 33. Biodiesel generator system
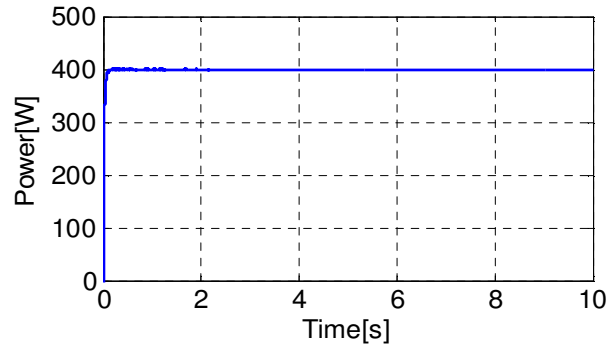
Figure 34. BDG output power

2.8 ENERGY SOURCES COUPLING AND CONTROL STRATEGY

The WECS and SPV work simultaneously as energy primary sources and the BDG as backup. In normal conditions, the WECS and the SPV provide the power to the load and charge the battery simultaneously with the excess power. If the wind and solar power delivered to the load is not sufficient because of low solar irradiance or low wind speed or when they stopped working, the battery delivers the power to the load with the energy stored previously. In worse situation where the battery discharges till the SOC reach a threshold of 45%, then the BDG is triggered automatically and start delivering the power to the load and charges the battery at the same time. The BDG start-up controller is developed with a hysteresis technique. Once started, the generator is not turned on till the battery SOC reaches 45%. The hysteresis distance is the difference between 85% and 45% and this prevents the BDG from turning on and off and vice-versa too often. When on, the BDG delivers the power to the load and charges the battery simultaneously. Current limitation is inserted at the battery input to limit the incoming current to the maximum in order to protect from overcharge and also protect its life span. The battery chosen in this paper is modeled by a variable voltage and a resistance representing the internal resistance. The battery SOC is calculated with the following equation

$$soc(\%) = soc_0(\%) + \frac{100}{Q} \int i_{out} \, dt \qquad (19)$$

where Q represents the battery capacity in Ampere hour and i_{out} is the instantaneous output current of the hybrid power system. The control strategy is illustrated by the flow chart presented in Figure 35.
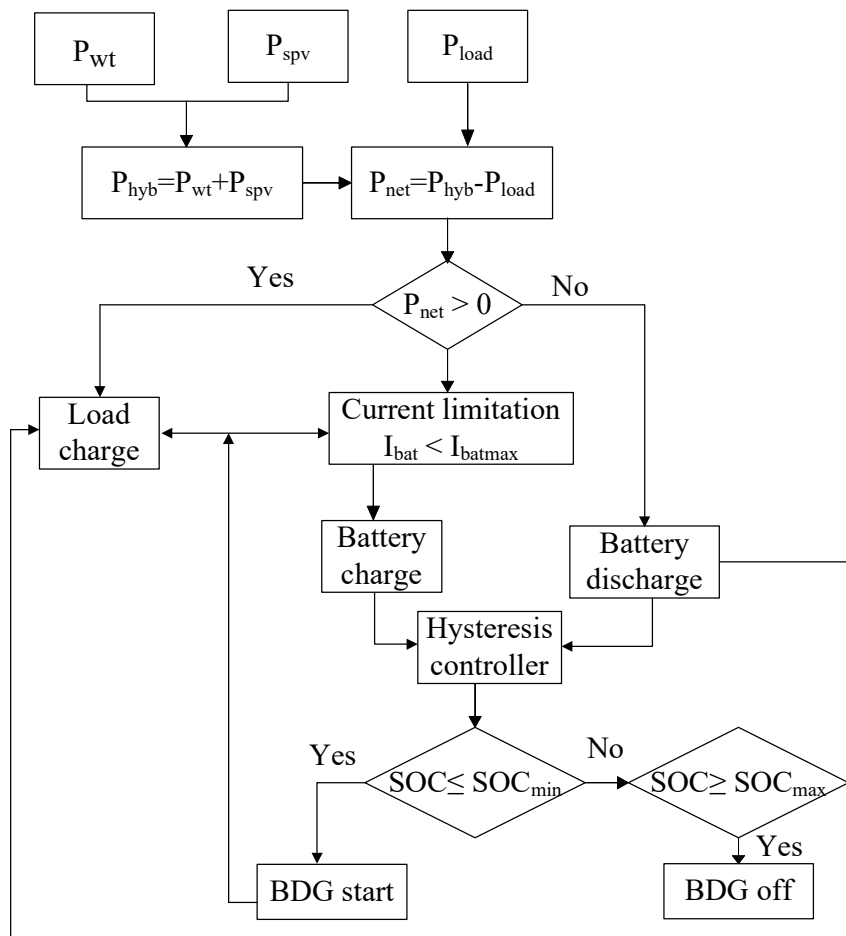
Figure 35. Hysteresis control strategy of the hybrid power system for the BDG

2.9 HPS SIMULATION AND DISCUSSION

The hybrid power system is simulated and analyzed according to two scenarios. The simulation is done within 20 seconds interval. Recall that the PV panel is 50 W, the wind turbine is 300 W, the BDG is 400 W and the rated load power consumption is 300 W. To reduce the simulation time which is very long in real case, the charging and discharging time of the battery is accelerated.

1) **First case**: the WECS works during the first 4 seconds and stops working the rest of time and the SPV works for 5 seconds and stops working. We assume that the battery is initially charged at 55%. The BDG is triggered only when the battery SOC decreases below 45%. Figure 36-a and Figure 36-b show the WECS output power and the SPV output power respectively. We observe in Figure 36-c that within 4 seconds the battery current is positive about 2 A which means that the battery is being charged. That is because the hybrid wind and solar output power is higher than the load power demand. As a result, the hybrid power system supplies power to the load and charges the battery simultaneously. Still, in Figure 36-c, it is seen that battery current has dropped about -10 A at 4 seconds and dropped again about -12 A at 5 seconds. That is due to the fact that at 4 seconds the WECS has stopped working and then at 5 seconds the SPV has also stopped working. Consequently, there is no power supply to the load, then the battery discharges to meet the load demand hence the battery current is negative. At 14.5 seconds, the battery current goes higher. That is due to the BDG that has been started up to feed the load and charges the battery. Figure 36-d explained clearly the battery SOC evolution. Compare to Figure 36-c, it can be seen that when the battery current is higher than zero, then the SOC increases and when it is lower than zero, the SOC decreases. Figure 36-e displays the BDG output power. It demonstrated that during the first 14.5 seconds the BDG is off and it was turned on immediately at 14.5 seconds. Figure 36-f illustrated that the hybrid power system is capable

of providing sufficient power to the load during the complete simulation time despite the variation of the wind and solar power.
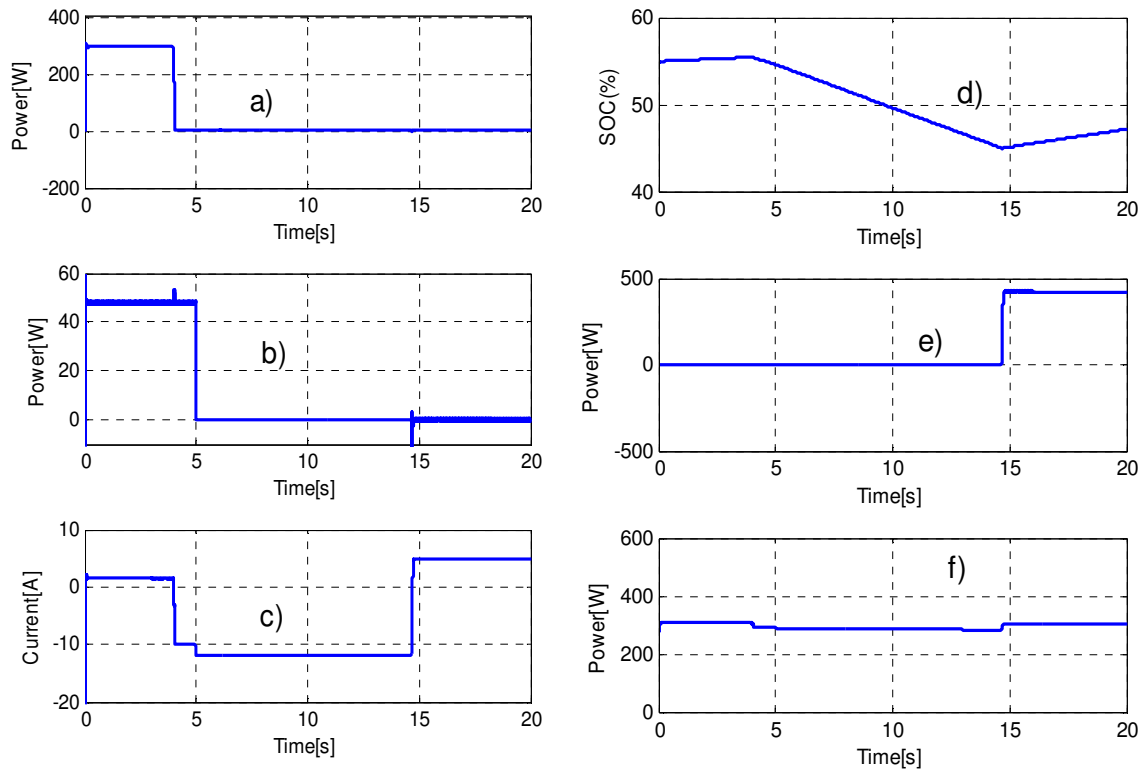
Figure 36. System response during the first case: (a) WECS power, (b) SPV power (c) battery current, (d) battery SOC, (e) BDG output power and (f) load power

2) **Second case**: the battery is initially charged at 55%, the WECS starts working after 4 seconds for 2 seconds and stops the rest of time, the SPV works during the first 8 seconds and stops working the rest of time. The BDG doesn't work at the beginning and it is supposed to work only if the battery SOC decreases below 45%. Figure 37-a and Figure 37-b show the WECS output power and the SPV output power respectively. Figure 37-c represents the battery output current. We observe that within 4 seconds, the battery current is -10 A which mean that the battery is being discharged. That is because during this time,

the WECS doesn't work and only the SPV supplies the power to the load. Since the load current requirement is higher than the SPV output, then the battery discharges to meet the load demand. After 4 seconds, the battery current has increased up to 2 A and keeps the same during 2 seconds which means that the battery is being charged. Actually, during this period the WECS has started working at its rated power and the total wind and solar power is higher than the load demand. Consequently, the hybrid wind and solar system supply the power to the load and charges the battery simultaneously. Between 6 seconds and 13 seconds, the battery output current has dropped again up to -12 A. This is explained by the fact that both the WECS and SPV have stopped working, so the battery discharges to meet the load demand. After 13 seconds and for the rest of time, the battery current has increased again. That is due to the backup BDG which has been started by the controller to supply the power to the load and charges the battery at the same time. Figure 37-d shows the battery SOC variation. In comparison to the battery current variation, we observe that when the battery current is negative, the SOC decreases and when it is positive the SOC increases. At 13 seconds, we can see that the SOC reaches 45% and has started increasing. Actually, as soon as the battery has reached the minimum SOC, then the backup BDG was triggered automatically to supply the power to the load and charges the battery simultaneously and Figure 37-e proves that the BDG has started at 13 seconds. In Figure 37-f, we observe that the load is sufficiently supplied by the hybrid system the whole time.

2.10 CONCLUSION

A hybrid power system integrating three renewable energy sources composed of wind, solar, biodiesel as well as a storage battery has been studied in this paper. The proposed method includes P&O algorithm to achieve the solar panels maximum power extraction and TSR technique to obtain the maximum power from the wind turbine. A hysteresis controller was used to trigger and stop automatically the backup BDG based on

the storage battery SOC level. The model shows that the load is always sufficiently supplied with power despite the variation of the wind speed and the solar irradiance. This hybrid system was analyzed through two scenarios based on the variation of the wind speed and the solar irradiance. The proposed system is intended to be installed in the renewable energy laboratory presented in [17] for educational purpose.
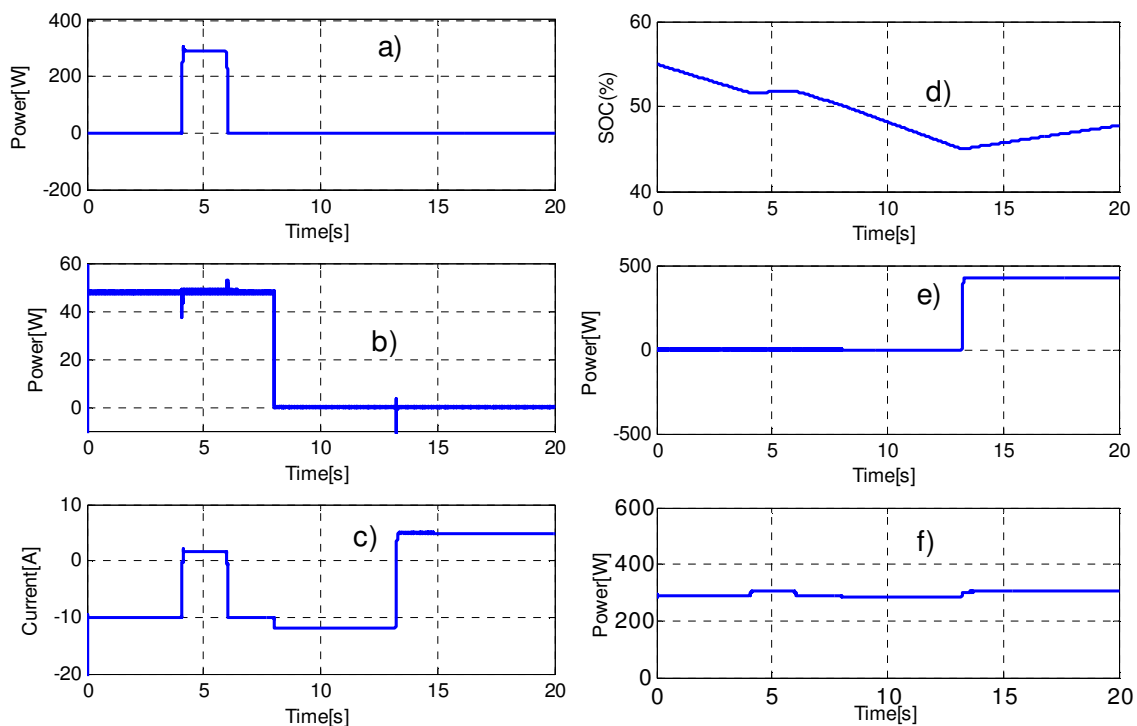

Figure 37. System response during the second case, (a) WECS power, (b) SPV power, (c) battery current (d) battery SOC, (e) BDG output power and (f) load power

2.11 REFERENCES

[1]   H. Sefidgar and S. A. Gholamian, "Fuzzy logic control of wind turbine system connection to pm synchronous generator for maximum power point tracking," Int. J. Intelligent Syst. and Appl., vol. 07, 2014

[2]   S. Singh, L. Mathew, and S.L. Shimi, "Design and simulation of intelligent control MPPT technique for PV module using MATLAB/ SIMSCAPE," Int. J. of Adv. Res. in Elect., Electro. and Instr. Eng., vol. 2, pp. 2278-8875, 2013.

[3]   N. A. Kamarzaman and C. W. Tan, "A comprehensive review of maximum power point tracking algorithms for photovoltaic systems," Renewable and Sustainable Energy Reviews, vol. 37, pp. 585-598, 2014.

[4]   A. Anurag, S. Bal, S. Sourav, and M. Nanda, "A comprehensible review of maximum power point tracking techniques for photovoltaic systems," Int. J. of sustainable energy, vol. 35, pp. 478-501, 2016.

[5]   M.-F. Tsai, C.-S. Tseng, and Y.-H. Hung, "A novel MPPT control design for wind-turbine generation systems using neural network compensator," IECON 2012-38th Annual Conf. on IEEE Indust. Elect. Soc., pp. 3521-3526, 2012.

[6]   M. A. Abdullah, A. H. M. Yatim, and C. Wei Tan, "A study of maximum power point tracking algorithms for wind energy system," IEEE First Conf. on Clean Energy and Tech. CET, pp. 321-326, 2011.

[7]   Y. Xia, K. H. Ahmed, and B. W.Williams, "A new maximum power point tracking technique for permanent magnet synchronous generator based wind energy conversion system," IEEE Trans. on power electronics, vol. 26, pp. 3609-3620, 2011.

[8]   E. M. Natsheh and A. Albarbar, "Hybrid power systems energy controller based on neural network and fuzzy logic," Smart Grid and Renewable Energy, vol. 4, pp. 187-197, 2013.

[9]   S. Kumar and V. K. Garg, "A hybrid model of solar-wind power generation system," Int. J. of Adv. Res. in Elect., Electro. and Instr. Eng., vol. 2, pp. 2278-8875, 2013.

[10]   C. Marisarla and K. R. Kumar, "A hybrid wind and solar energy system with battery energy storage for an isolated system," Int. J. of Eng. and Innov. Tech., 2013.

[11]   S. Alsadi and B. Alsayid, "Maximum power point tracking simulation for photovoltaic systems using perturb and observe algorithm," Int. J. of Eng. and Innov. Tech., vol.2, Issue 6, 2012.

[12]   S. Heier, Grid integration of wind energy conversion systems, 2nd ed. Chichester, England: J. Wiley, 2006.

[13]   Y. S. Rao, A. J. Laxmi, and M. Kazeminehad, "Modeling and control of hybrid photovoltaic wind energy conversion system," Int. J. of Adv. in Eng. and Tech., pp. 2231-1963, 2012.

[14]   M. M. K. Bhuiya, M. G. Rasul, M. M. K. Khan, N. Ashwath, A. K. Azad, and M. A. Hazrat, "Prospects of 2nd generation biodieselas a sustainable fuel – Part2: Properties, performance and emission characteristics," Renewable and Sustainable Energy Reviews, vol. 55, pp. 1129–1146, 2016.

[15]   S. Tang, G. LaDuke, W. Chien, and B. P. Frank, "Impacts of biodiesel blends on PM2.5, particle number and size distribution, and elemental/organic carbon from nonroad diesel generators," Fuel, vol. 172, pp. 11-19, 2016.

[16]   J. Yanga, C. Caldwellb, K. Corscaddena, Q. S. Hea, and J. Li, "An evaluation of biodiesel production from Camelina in Nova Scotia," Industrial Crops and Products, vol. 81, pp. 162-168, 2016.

[17]   M. Soro, A. Chebak, and N Barka, "Development of renewable energy laboratory based on integration of wind, solar and biodiesel energies through a virtual and physical environment," 3rd Int. Renewable and Sustainable Energy Conf. (IRSEC), pp. 1 - 8, 2015.

CHAPITRE 3

DÉVELOPPEMENT D'UN CONTRÔLE EFFICACE BASÉ SUR LA LOGIQUE FLOUE POUR ÉOLIENNE ET PANNEAUX SOLAIRES INTÉGRÉS DANS UN SYSTÈME D'ÉNERGIE HYBRIDE

3.1   RESUME EN FRANÇAIS DU TROISIEME ARTICLE

Cet article présente la simulation et l'implantation d'une méthode de contrôle, basée sur la logique floue, d'un système d'énergie hybride intégrant un système de conversion d'énergie éolienne, un système solaire photovoltaïque, une génératrice au biodiesel ainsi qu'une batterie de stockage. Des systèmes de contrôle basés sur la logique floue sont étudiés, analysés et appliqués au système éolien et au système solaire photovoltaïque pour extraire efficacement les puissances maximales. Dans le système solaire, le contrôleur flou est implanté, analysé et comparé au contrôleur de type Perturber et Observer (P&O) à travers l'analyse de la puissance de sortie. Dans le système éolien, le contrôleur flou est comparé au système de contrôle de la vitesse spécifique de la turbine (Tip Speed Ratio : TSR). Ainsi, les puissances de sortie mécanique et électrique, et le coefficient de puissance de la turbine éolienne sont comparés en utilisant les deux systèmes de contrôle. Le système de la génératrice au biodiesel est également présenté brièvement. Ensuite, le couplage des trois sources d'énergie est effectué et analysé via deux scénarios pour montrer la fiabilité du système proposé à fournir une puissance suffisante à la charge en tout temps. Un contrôleur par hystérésis est utilisé pour déclencher et arrêter la génératrice au biodiesel et maintenir également la variation de l'état de charge de la batterie de stockage (SOC) entre les valeurs désirées. Les résultats des simulations démontrent que les contrôleurs flous permettent de suivre les points de puissance maximaux plus efficacement que les systèmes de contrôle de

type P&O et TSR. De plus, les résultats montrent que le couplage de trois sources d'énergie permet d'augmenter la fiabilité de la puissance malgré les variations de la vitesse du vent et des radiations solaires.

Le but du troisième article était d'étudier le fonctionnement des sources d'énergie solaire et éolienne commandées par des contrôleurs flous. Ainsi, pour faire notre analyse, nous avons fait les comparaisons des résultats des simulations du système solaire et du système éolien fonctionnant avec des commandes de type MPPT en utilisant, d'une part, des contrôleurs de logique floue, et d'autre part, des contrôleurs de type P&O et TSR. Après l'étude du système solaire et éolien, nous avons brièvement présenté la génératrice au biodiesel utilisée comme source d'énergie de secours dans le système hybride, puis nous avons couplé les trois sources débitant sur une batterie de stockage et une charge DC. L'étude du système hybride complet a été faite suivant deux scénarios basés sur les variations des radiations solaires et de la vitesse du vent.

Ce troisième article intitulé « Efficient fuzzy logic MPPT control for solar panel and wind turbine in hybrid power system » fut rédigé par moi-même. En tant que premier auteur, j'ai fait la recherche sur l'état de l'art puis développé la méthode de travail et rédigé l'article. Le professeur Ahmed Chebak, second auteur, a fourni l'idée originale et a aidé à la recherche sur l'état de l'art au développement de la méthode ainsi qu'à la révision de l'article. Les professeurs Abderazak El Ouafi et Mustapha Mabrouki ont contribué avec leurs commentaires sur la méthode adoptée et ont participé à la révision de l'article. Cet article sera soumis à un journal scientifique.

3.2 EFFICIENT FUZZY LOGIC MPPT CONTROL FOR SOLAR PANEL AND WIND TURBINE IN HYBRID POWER SYSTEM

ABSTRACT

This paper presents the simulation and the implementation of an efficient control method, based on fuzzy logic (FL) technique, of a hybrid power system (HPS) integrating a wind energy conversion system (WECS), a solar photovoltaic system (SPV) and a biodiesel generator (BDG) as well as a storage battery. Fuzzy logic (FL) Maximum Power Point Tracking (MPPT) control systems are studied, analyzed and applied to the SPV and to the WECS to efficiently extract maximum power. In the SPV, the FL technique is compared to Perturb and Observe (P&O) algorithm through the output power analysis. In the WECS, the FL technique is compared to the Tip Speed Ratio (TSR) technique. The mechanical and the electric output power, and the power coefficient of the wind turbine (WT) are presented and analyzed using both FL and TSR MPPT control. The BDG system is briefly presented. Afterwards, the coupling of the three energy sources is performed and analyzed via two scenarios to show the reliability of the proposed system to continuously providing sufficient power to the load. A hysteresis controller is used to trigger and stop the backup BDG and also to maintain the storage battery state of charge (SOC) variation between the desired values. The simulations results demonstrate that the FL MPPT controllers permit to track the maximum power point of SPV and WT more efficiently in comparison to traditional techniques such as P&O and TSR controllers. Moreover, the results show that coupling of three energy sources helps to increase power reliability despite the wind speed and solar irradiance variation.

Keywords—Fuzzy logic; MPPT; hybrid power system; renewable energy, wind and solar energies, Perturb and Observe; Tip Speed Ratio; SOC.

3.3 INTRODUCTION

Due to the climate change rapid progress caused by the fossil fuels, renewable energy has made an impressive development worldwide. Actually, renewable energy is clean, environmentally friendly and don't releases greenhouses gases like the fossil fuels. Among the renewable energies, the solar and wind energies are the most attractive because they offer many advantages. The wind energy doesn't necessitate fuel cost and requires low maintenance [1]. As for the solar photovoltaic, it requires low fuel cost and little maintenance and does not make noise [2].

However, the wind and solar energy systems are highly unreliable due to their unpredictable nature [3]. Actually, they are mainly dependent on solar radiation and wind speed, which are variable and difficult to predict. Moreover, the wind turbine (WT) and solar panels efficiencies are a key issue that needs to be taken into consideration because they are non-linear systems. The solar panels have current-voltage (I¬V) and power-voltage (P-V) characteristics which vary with the solar radiation and the temperature [4]. The wind turbine has a mechanical power-rotor speed characteristic which varies according to the wind speed. Both systems have some peak power points that need to be tracked to extract the maximum power. This process is known as Maximum Power Point Tracking (MPPT) and it is performed by a MPPT controller. The amount of power extracted depends on the accuracy of the MPPT controller.

Many MPPT controllers have been implemented and published in the literature. For the wind energy conversion system, the Tip Speed Ratio (TSR), the Power Signal Feedback (PSF), and the Perturb and Observe (P&O) algorithms are some of them. The TSR control is a simple control method used to regulate the wind turbine rotation speed in order to maintain an optimal value of TSR. However, with this method, the rotor speed doesn't adapt itself quickly with wind turbine parameters change in order to keep the optimal TSR [5]. The PSF is also another method which is used to extract the maximum power.

However, it requires the knowledge of the wind turbine maximum power curve which the control system tracks in order to deliver the maximum point. Hill-climb Search (HCS), especially the perturb and observe (P&O) method, is one of the most used method because it is easy to implement. It consists of continuously searching the peak power point of the wind turbine. However, this method has a low tracking performance and presents many oscillations around the maximum point [6, 7]. As for the solar panels, the P&O, the incremental capacitance, the constant voltage are among the MPPT techniques used to extract maximum power of the solar PV panels. However, these methods have difficulty like severe oscillations around the maximum point, and are costly, difficult to implement and non-stable [8, 9]. To overcome these traditional MPPT control systems challenges, intelligent controllers such as Fuzzy Logic (FL) and Artificial Neural Network (ANN) have been introduced in recent years by scientists.

The solar and wind energies are complementary in nature. During sunny days, the wind will be most of the time weak and generally strong wind will blow during nights and cloudy days. Hence, coupling the two energy sources can increase the power reliability [10]. However, in worse weather condition where the wind speed and the solar irradiance become weak, the power supply may be seriously affected.

The objective of this article is to present an efficient control method based on fuzzy logic technique to extract maximum power from solar panels and wind turbine used in a hybrid power system (HPS) integrating three energy sources. The HPS includes a solar photovoltaic system (SPV), a wind energy conversion system (WECS) and a biodiesel generator (BDG) as well as a storage battery and DC load. The fuzzy logic is chosen because of its adaptive capability to parameters change and its robustness. It is more stable also relatively simple to design since it doesn't require information about the exact model [11]. The three energy sources permit to provide uninterrupted power supply under all weather conditions.

The paper is organized as follows: the complete hybrid power system architecture is first presented, and then the SPV and the WECS functioning are simulated and studied through comparison between FL and P&O MPPT control system and between FL and TSR control system respectively. The BDG is also briefly presented. Afterwards, the coupling working principle of the three energy sources is presented and the control strategy of the complete system is performed. Finally, the simulation results are discussed and analysed through two scenarios.

3.4 HYBRID POWER SYSTEM

The proposed hybrid power system consists of SPV, WECS, BDG, storage battery, DC-DC converters and DC load. The architecture is presented in Figure 38. The SPV and the WECS work as primary source to provide power to the load and charge the battery simultaneously. The BDG is a backup source and work only when the battery is below a minimum charge. A hysteresis controller is used to start and stop the BDG and to maintain the battery state of charge (SOC) variation between a minimum of 40% and maximum value of 80%. The electrical rated power of all components used in this study is as follow: the wind turbine is 300 W, the solar panel is 50 W, the biodiesel generator is 400 W, the battery capacity is 200 Ah-24 V and the DC load is 300 W.

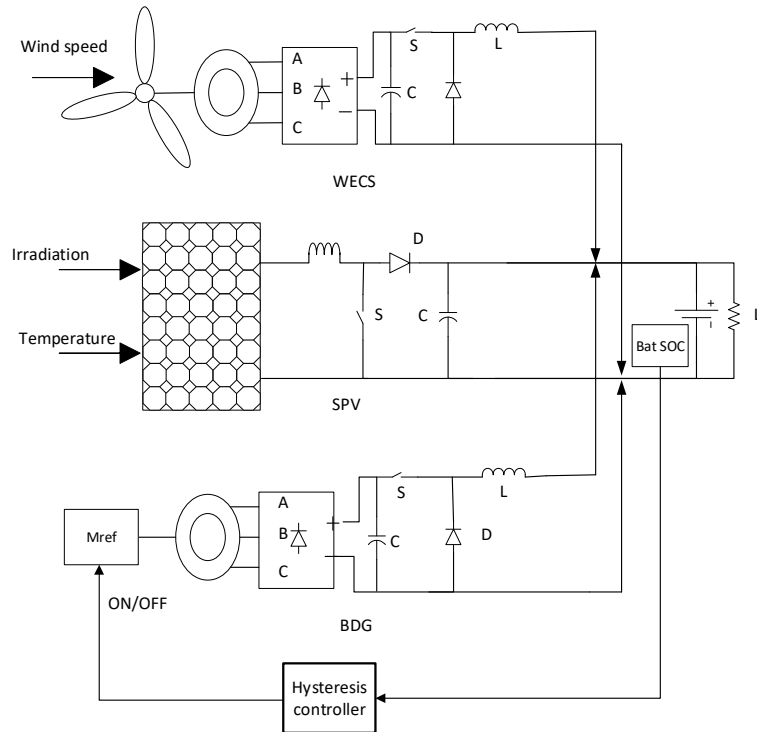**Figure 38. Complete hybrid power system**

3.5   SOLAR PHOTOVOLTAIC SYSTEM

3.5.1   SPV electrical components

The SPV is composed of solar PV, boost converter, fuzzy logic control system, storage battery and DC load. It is presented in Figure 39.
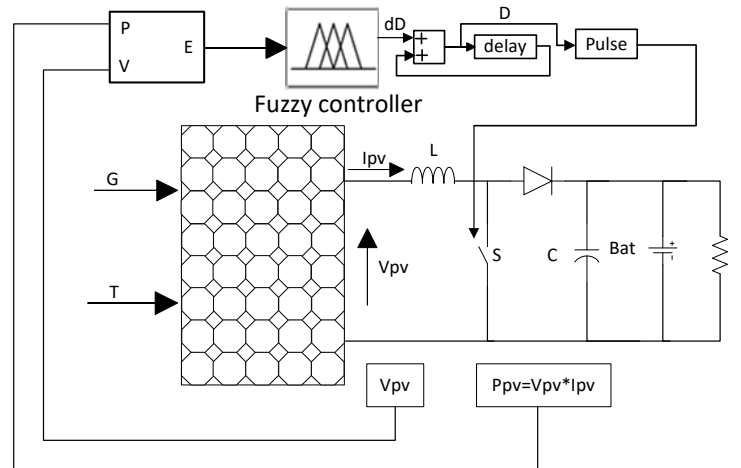
Figure 39. SPV system with FL MPPT control system

3.5.2 SPV fuzzy logic MPPT controller

The purpose of the MPPT controller is to track and extract maximum power from PV panels for a given solar irradiance. The MPPT control system applied to our SPV is based on fuzzy logic algorithm. It is a non-linear control method which attempt to apply the expert knowledge of an experienced user to the design of a fuzzy-based controller. Generally, it is composed of four main components as shown in Figure 40.

− The fuzzifier that maps crisp values into input fuzzy sets to activate rules. This process is the fuzzification.

− The rules which define the controller behavior by using a set of IF-THEN statements.

− The inference engine which maps input fuzzy sets into output fuzzy sets by applying the rules.

− The defuzzifier that maps output fuzzy values into crisp values. This process is the defuzzification [12].
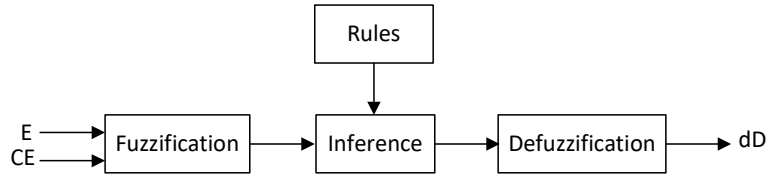
Figure 40. Structure of fuzzy logic

The proposed method permits to address the oscillations issue of fixed step size methods such as P&O algorithm. One input variable namely error (E) which correspond to dP/dV is used. It is expressed as follow

$$E(k) = \frac{P(k) - P(k-1)}{V(k) - V(k-1)} \tag{20}$$

Where P and V are the solar PV power and voltage respectively and k is the sampling instant. Based on the solar panels P¬V characteristic shown in Figure 41, the maximum power is reached when $E(k)$ (i.e. dP/dV) is zero. When the PV operating point is on the left side of the PV MPP (i.e. dP/dV is higher than zero), then the FL MPPT controller decreases the duty cycle (D) to force the PV operating point to move to the MPP. Similarly, if the operating point is on the right side of the MPP (i.e. dP/dV is less than zero, then the FL MPPT controller increases the duty cycle to forces the PV operating point to move to the MPP. According to the fuzzy logic technique, the input variables are expressed in terms of linguistic variables such as NB (negative big), NS (negative small), ZO (zero), PS (positive small), PB (positive big) using fuzzy subset. The output variable used is the change of duty ratio (dD). The membership grades of fuzzy subset for input and output variables are displayed in Figure 42-a and Figure 42-b and the fuzzy rules viewer is presented in Figure 43. The control fuzzy rules are also presented in Table 6.
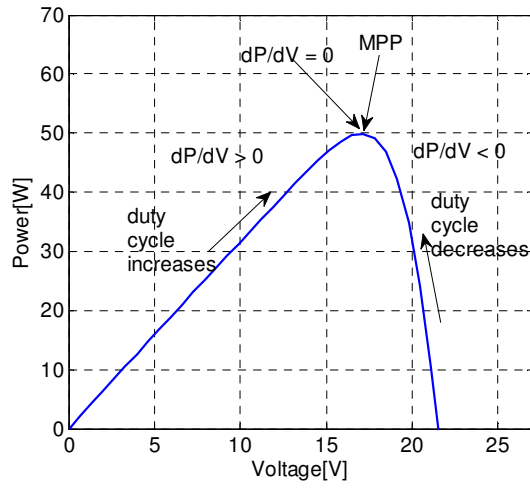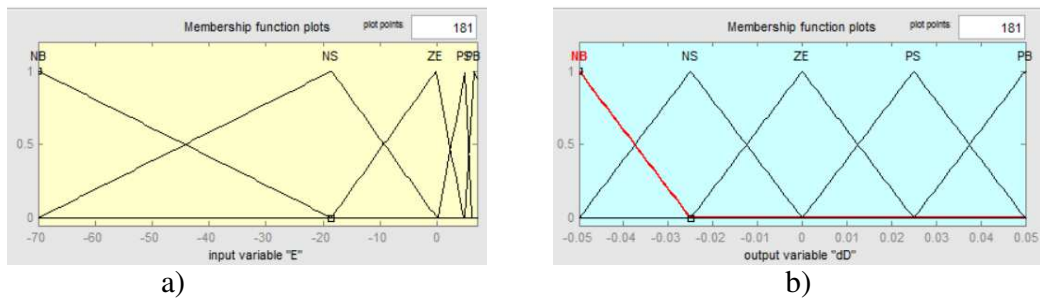
Figure 41. Solar PV power versus voltage

| a) | b) |

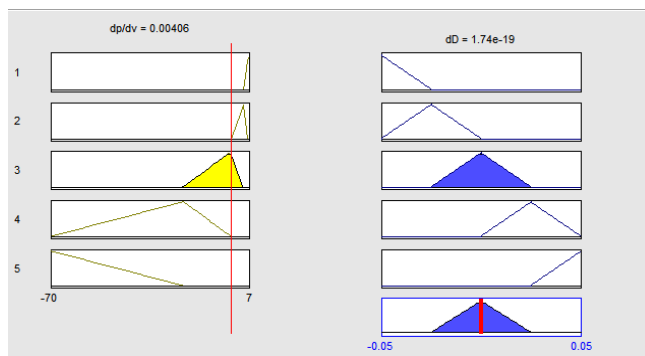**Figure 42. Membership function for (a) input *E* and (b) output d*D***

Figure 43. Fuzzy rules viewer

Table 6. Control fuzzy rules for the SPV

Input dP/dV	Output dD
NB	PB
NS	PS
ZO	ZO
PB	NB
PS	NS

An illustrated example of control rule in Table 6 is : If dP/dV is PS then dD is NS. This implies that 'if operating point is closed to maximum power point towards right hand side, then decrease duty ratio a little'. Fuzzy inference methods are classified in direct methods and indirect methods. Direct methods include Mamdani's and Sugeno's. There are the most commonly used and they only differ in how they obtain the outputs. Indirect methods are more complex. The fuzzy control uses one of the following methods: max-min, max-prod, sum-prod inference technique [13, 14]. The Mamdani inference method which is a max-min fuzzy combination law is chosen in this paper because it is intuitive and has widespread acceptance. After the inference process, the defuzzification is used to transform the fuzzy subsets of control from the fuzzy output controller into non-fuzzy value of control. There are two algorithms that can be used to perform the defuzzification: the Center of Area (COA) and the Max Criterion Method (MCM). The algorithm uses in this paper is the COA which is the most used in the world. It is a combine-then-defuzzification algorithm that determines the crisp controller output as the center of gravity of the final combined fuzzy set. The final combined fuzzy set is defined by the union of all rule output fuzzy set using the maximum aggregation method. For a sampled data representation, the center of gravity dD is computed point-wise by:

$$dD_0 = \frac{\sum\limits_{j=1}^{n} \mu(D_j).D_j}{\sum\limits_{j=1}^{n} \mu(D_j)} \qquad\qquad (21)$$

3.5.3   SPV simulation results and discussion

To better evaluate the FL MPPT control system performance, the simulations results are compared with a P&O MPPT control system. The applied solar irradiance profile is seen in Figure 44-a. Figure 44-b displays the solar panel output power which correspond to the boost converter input power (Pin) and the boost converter output power (Pout). We observe that both are identical. This means that FL MPPT is able to extract the maximum power from the solar panels. Moreover, in Figure 44-c, the obtained solar output voltage is around 17.2 V which correspond to the voltage at the maximum power. Comparing FL MPPT to P&O, Figure 45 proves that the PV system boost converter output power (Pout--FL) is more stable when using FL, whereas with P&O severe power oscillations (Pout--P&O) around the MPP occurs, which will eventually lead to power loss problem in the PV.
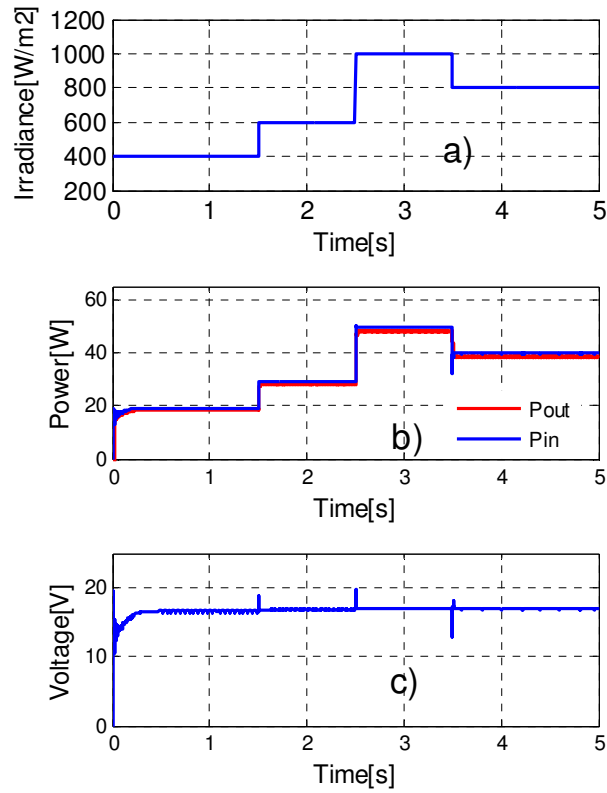
Figure 44. a) Solar irradiance profile, b) DC-DC converter input power and output power, and c) SPV voltage
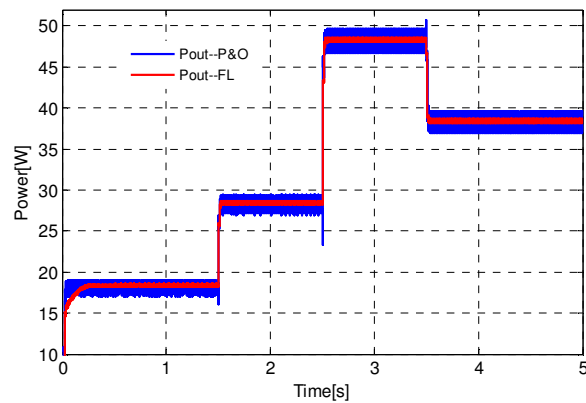

Figure 45. Comparison between DC-DC converter output power with P&O MPPT and FL MPPT

3.6 WIND ENERGY CONVERSION SYSTEM

3.6.1 WECS electrical components

The WECS is composed of wind turbine, Permanent Magnet Synchronous Generator (PMSG), diode bridge rectifier, buck converter, fuzzy logic control system, storage battery and DC load. The complete system is presented in Figure 46.
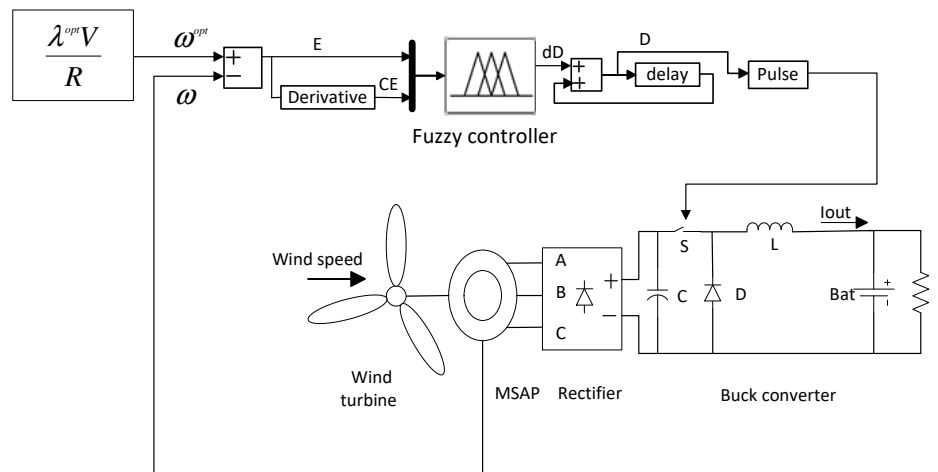
Figure 46. WECS system with FL MPPT control system

3.6.2 WECS fuzzy logic MPPT controller

As a non-linear system, the wind turbine doesn't always work in optimal condition. Therefore, a MPPT controller is needed to track the MPP according to the wind speed. In this paper, the FL control system is adopted. It is used to vary the duty cycle (*D*) of the DC-DC converter to track the optimum rotor speed, thus maximizing the extracted power from the wind turbine. The adopted FL controller has two inputs and one output. The two inputs are the error between the actual rotor speed and the optimal reference rotor speed namely *E* and the change of the error namely *CE*. The output is the duty cycle of the converter to

achieve optimal rotor speed namely d*D*. The input variables are expressed in terms of linguistic variables such as NB (negative big), NS (negative small), ZO (zero), PS (positive small), and PB (positive big) using fuzzy subset. The output variable used is the change of duty ratio (d*D*(*k*)), thus $D(k) = D(k\text{-}1) + dD(k)$. The membership grades of fuzzy subset for input and output variables are displayed in Figure 47 and the control surface for the FL model is plotted and represented by a 3D curve in Figure 48.
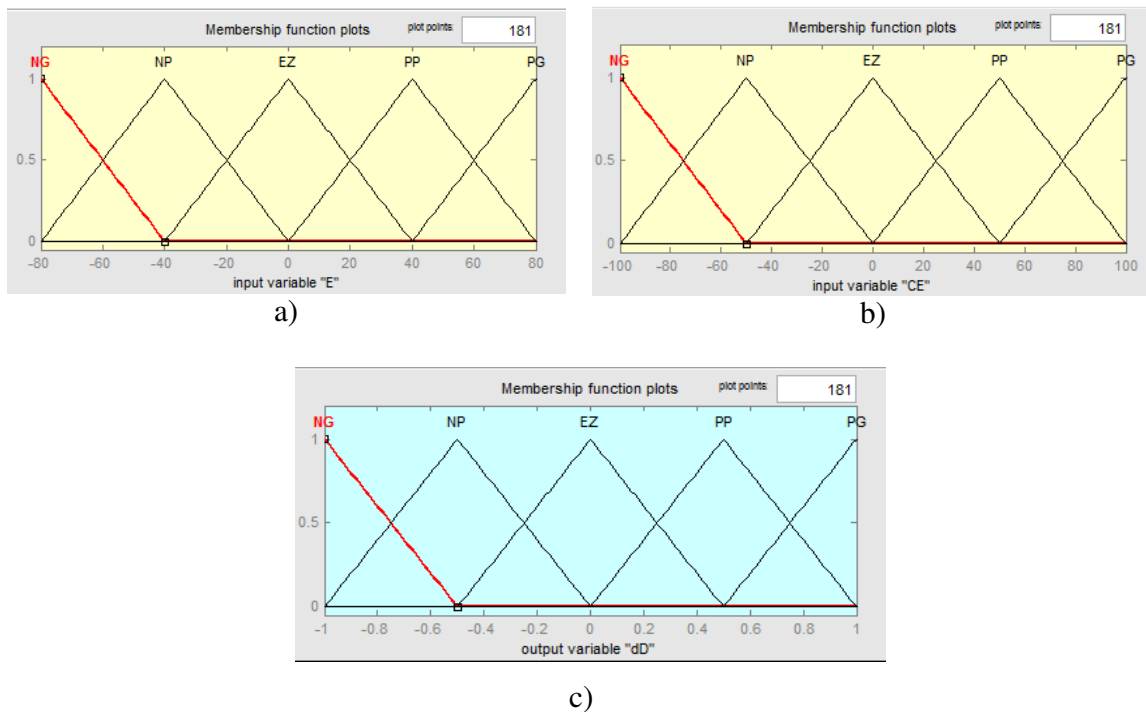

a)

b)

c)

Figure 47. Membership function for (a) input *E*, (b) input *CE* and (c) output d*D*
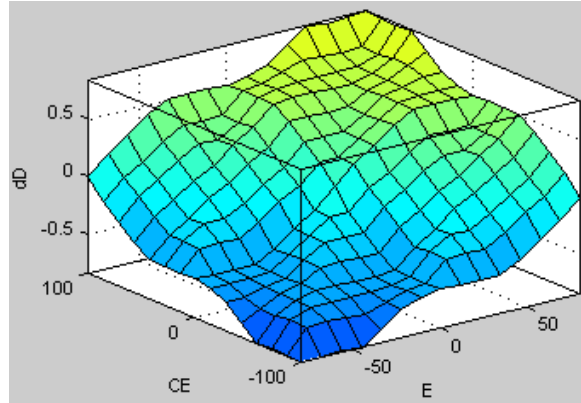
Figure 48. FLC model control surface with input *E* and *CE* and output d*D*

The steps to get the reference optimum rotor speed are described as follow. The mechanical power provided by wind turbine is given by the equation

$$P_w = \frac{1}{2}\rho C_p(\lambda, \beta)AV^3 \qquad (22)$$

where ρ is the air density, A is the swept area of the rotor blade, it is equal to πR^2, V is the wind speed and $C_p(\lambda, \beta)$ is the power coefficient. The power coefficient determines the efficiency of the wind turbine depending on the Tip Speed Ratio (λ) and the pitch angle (β). The evolution of the power coefficient is presented in Figure 49 where it clearly appears that the maximum power coefficient is 0.48 for $\lambda = 8$ and $\beta = 0$. Parameter λ stands for the ratio between turbine speed and the wind speed. It is given by the equation

$$\lambda = \frac{\omega R}{V} \qquad (23)$$
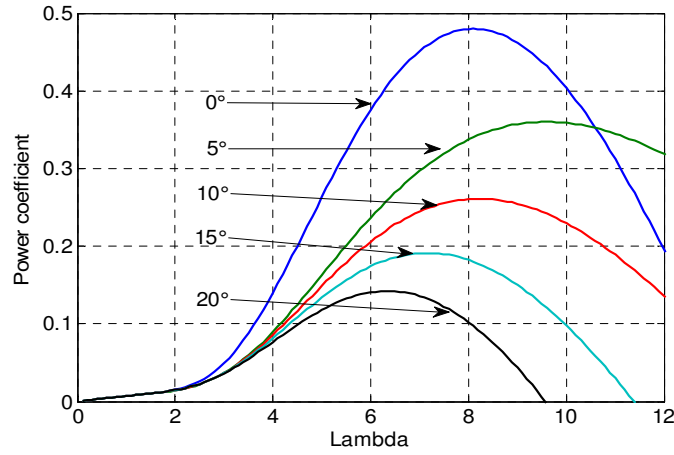
Figure 49. WT power coefficient versus the tip speed ratio λ (lambda) for different values of the pitch angle β

The optimal wind turbine power is obtained when the power coefficient $C_p(\lambda,\beta)$ is maximum which corresponds to β equal zero and λ is optimum. Generally λ is optimum for a value around 8 and 9. If λ is maintained at the optimal value, then the wind turbine maximum power is

$$P^{opt} = \frac{1}{2}\rho C_p(\lambda^{opt})AV^3 \tag{24}$$

and the optimum tip speed ratio is given by

$$\lambda^{opt} = \frac{\omega^{opt}R}{V} \tag{25}$$

From equation (25), we obtained the optimum rotor speed as follow

$$\omega^{opt} = \frac{\lambda^{opt}V}{R} \tag{26}$$

The control fuzzy rules are presented in Table 7 where E is the error between the optimal rotor speed and the actual one, CE the variation of the error and the output is the duty ratio dD of the converter.

Table 7. Control fuzzy rules for the WECS

E\CE	NB	NS	ZO	PS	PB
NB	NB	NB	NS	NS	ZO
NS	NB	NS	NS	ZO	PS
ZO	NS	NS	ZO	PS	PS
PS	NS	ZO	PS	PS	PB
PB	ZO	PS	PS	PB	PB

3.6.3 WECS simulation results and discussions

The proposed WECS was simulated with a variable wind speed using a fuzzy logic controller compared to the TSR technique. The results are displayed and analyzed in this section. The wind speed profile is shown in Figure 50-a and in Figure 50-b, we observe that the wind turbine mechanical output power (*WTP*) follow the optimal power (P_{opt}), which means that FL controller is capable of extracting the maximum power from the wind turbine. In addition, it clearly appears in Figure 50-c that the obtained power coefficient is around 0.48, which corresponds to the maximum power coefficient of the turbine. For a better analysis of the WECS, the power coefficient and the electrical power of the wind turbine are compared using FL and TSR control technique. In Figure 51-a, it is seen that with FL, the power coefficient (C_P-FL) is slightly higher compared with TSR (C_P-TSR) and both are around the maximum power coefficient (C_P-max). Actually, during wind speed changes, with FL MPPT, the WT quickly adapts its rotation speed to provide the maximum power compared to the TSR control. As illustration, Figure 51-b shows that the WECS electrical power obtained with the FL and TSR MPPT is almost the same. However, with

FL MPPT, the electrical power (P_{out}-FL) is 4 % higher than with TSR MPPT (P_{out}-TSR). In other words, the FL MPPT accurately extracts the maximum power from the wind turbine compared to TSR MPPT especially during the wind speed change.
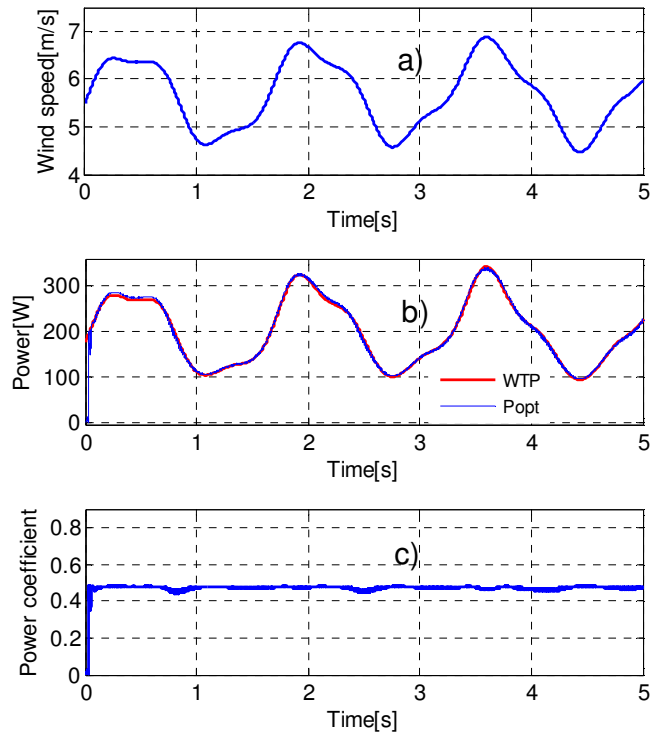

Figure 50. a) Wind speed profile, b) WT mechanical optimal and extracted power, and c) WT power coefficient for the FL controller
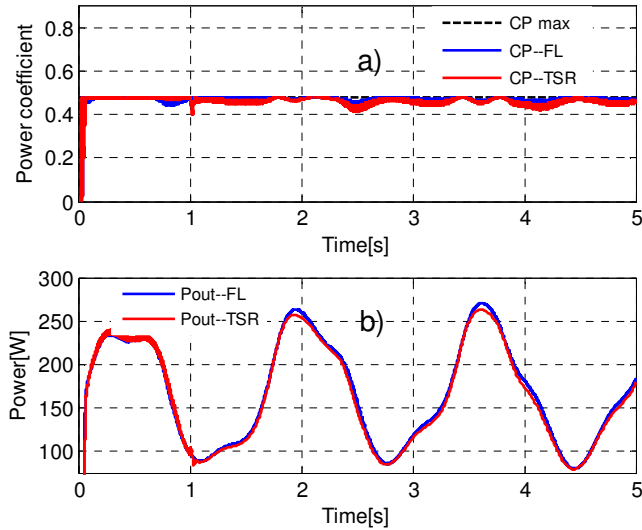
Figure 51. a) Comparison between WT maximum power coefficient and power coefficient using FL and TSR control, and b) comparison between the WECS electrical output power for FL and TSR

3.7 BIODIESEL GENERATOR SYSTEM

The biodiesel generator system includes biodiesel motor, PMSG, rectifier, buck converter, battery, DC load, and output current regulation system. The BDG system is presented in Figure 52. The output current is regulated with the rated output current taken as reference current. The generator is fueled with biodiesel. In order to save the fuel cost, the BDG is used as backup and work only in worse case, when the WECS, the SPV and the storage battery couldn't meet the load requirement. The rated output power of the BDG obtained from the system simulation is presented in Figure 53.
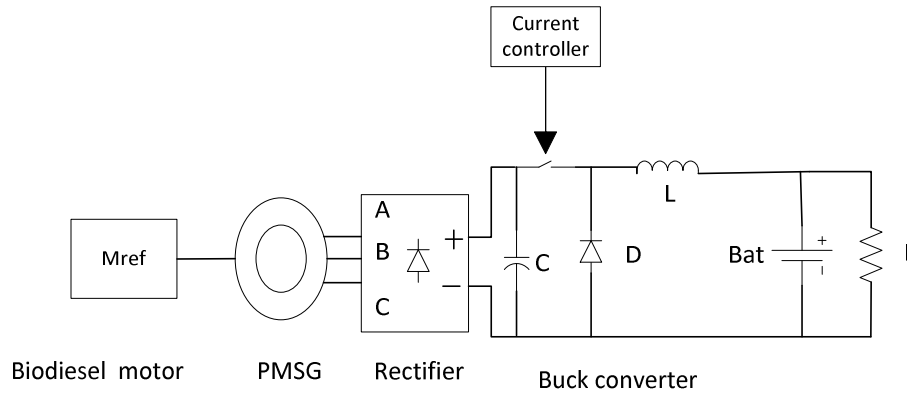
Figure 52. Biodiesel generator system
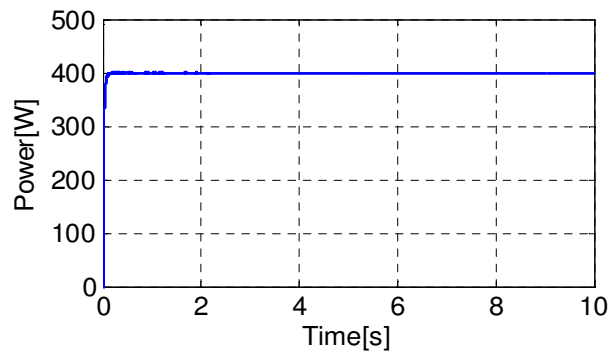
Figure 53. BDG output power

3.8 HPS CONTROL SYSTEM AND SIMULATION

The hybrid power system is composed of SPV, WECS, Biodiesel generator, storage battery and DC load. The SPV and WECS work as primary sources. These systems provide the power to the load and store the remaining power in the battery. When the power delivered by both the WECS and the SPV is not sufficient for the load, then the stored energy in the battery is delivered to the load, which causes the battery SOC decreasing. The BDG is used as backup and work only in worse case when the battery SOC is very low. A hysteresis controller is used for the BDG start-up and stop in order to maintain the battery

SOC between 40% and 80%. However, for simulation purpose and in the aim of highlighting the battery SOC evolution in a short time simulation, the battery SOC evolution is limited between 53% and 55%. The HPS is simulated in 5 second interval and two cases are studied below.

1) **First case**: in this case, the WECS works between 1 second and 2 seconds and remains down the rest of time and the SPV works between 2 seconds and 3 seconds and remains down the rest of time as displayed in Figure 54-a and Figure 54-b. In Figure 54-c, we observe that between 0 second and 1 second the battery current is lower than 0 (-12 A), and between 1 second and 2 seconds the current increases to 2.2 A. Between 2 seconds and 3 seconds, the battery current gets down to -10 A and decreases a little to almost -12 A. At 3.3 second, the current increases again to 4 A. Actually, between 0 second and 1 second the WECS and SPV are down, which causes the battery providing the power to the load. Consequently, the battery discharges and the current gets lower than zero. At 1 second, the WECS starts, so it delivers the power to the load and charges the battery simultaneously. This explained why the battery current increases at this time. At 2 seconds, the WECS stops and the SPV starts. Between 2 seconds and 3 seconds, the current is -10 A because only the SPV provide the power to the load. However, the power delivered can't meet the load power requirement, and then the battery discharges again to provide the remaining power. At 3 seconds, the battery current decreases again a little because the SPV stops, so the battery provides additional power to meet the load power requirements, which causes the current in decreasing again. The current increases again at 3.3 second to 4 A due to the fact that the battery SOC reaches the fixed minimum SOC of 53% as seen in Figure 54-d, therefore the BDG starts at this point as displayed in Figure 54-e. Then BDG delivers the power to the load and charges the battery, thus the current increases. By comparing Figure 54-c and Figure 54-d, it appears that when the battery current decreases then the SOC decreases, and when the current increases then the SOC increases. The Figure 54-f proves that during the complete simulation time, the load is sufficiently provided with power.
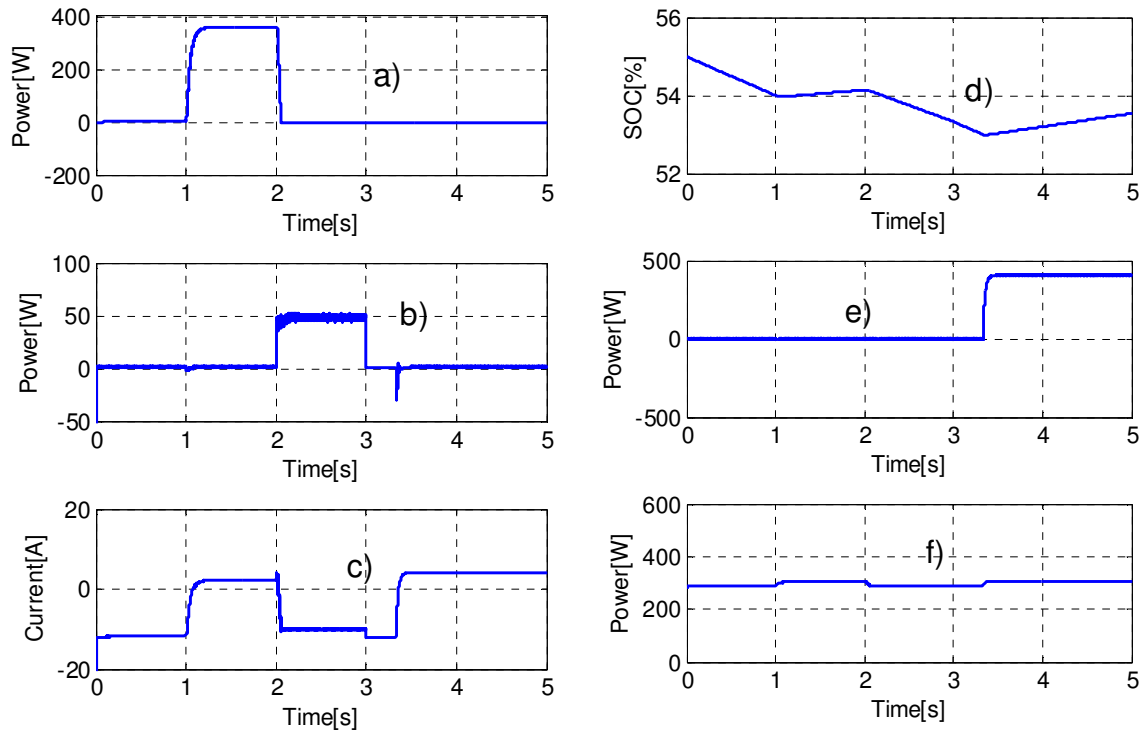
Figure 54. HPS response during the first case: (a) WECS power, (b) SPV power, (c) battery current, (d) battery SOC, (e) BDG power and (f) load power

2) **Second case**: in this case, the wind turbine works between 2.5 seconds and 3.5 seconds and gets down the rest of time, and the solar system works between 1.5 seconds and 2.5 seconds and gets down the rest of time as seen in Figure 55-a and Figure 55-b, respectively. In Figure 55-c, we observe that the battery current is lower than 0 (-12 A) between 0 second and 1.5 seconds, and increases to 6.3 A from 1.6 seconds to 2.5 seconds and then increases again till 15.5 A. At 3.5 seconds, the current drops down lower than zero (about -12 A). Actually, during 0 second and 1.5 seconds the wind turbine and the solar system don't work, so only the battery provides energy to the load. This causes the battery discharging and the current decreasing. Between 1.6 seconds and 2.5 seconds the battery current increases to 6.3 A because at 1.6 seconds the battery SOC reaches the minimum threshold of 53% as illustrated in Figure 55-d, which causes the BDG to start as displayed

in Figure 55-e. Then, the BDG delivers the power to the load and charges the battery simultaneously. Between 2.5 seconds and 3.5 seconds, the battery current increases again because the wind turbine starts at 2.5 seconds, which leads to additional power to the battery. At 3.5 seconds, the battery current drops lower than zero around -12 A. This is due to the fact that the wind turbine stops when the battery SOC reaches the fixed maximum SOC of 55%, so the BDG stops as seen in Figure 55-d and Figure 55-e. The Figure 55-f proves that the load is sufficiently powered about 300 W during the whole 5 second interval of simulation despite the fact that the wind and solar energies are very low and vary a lot.
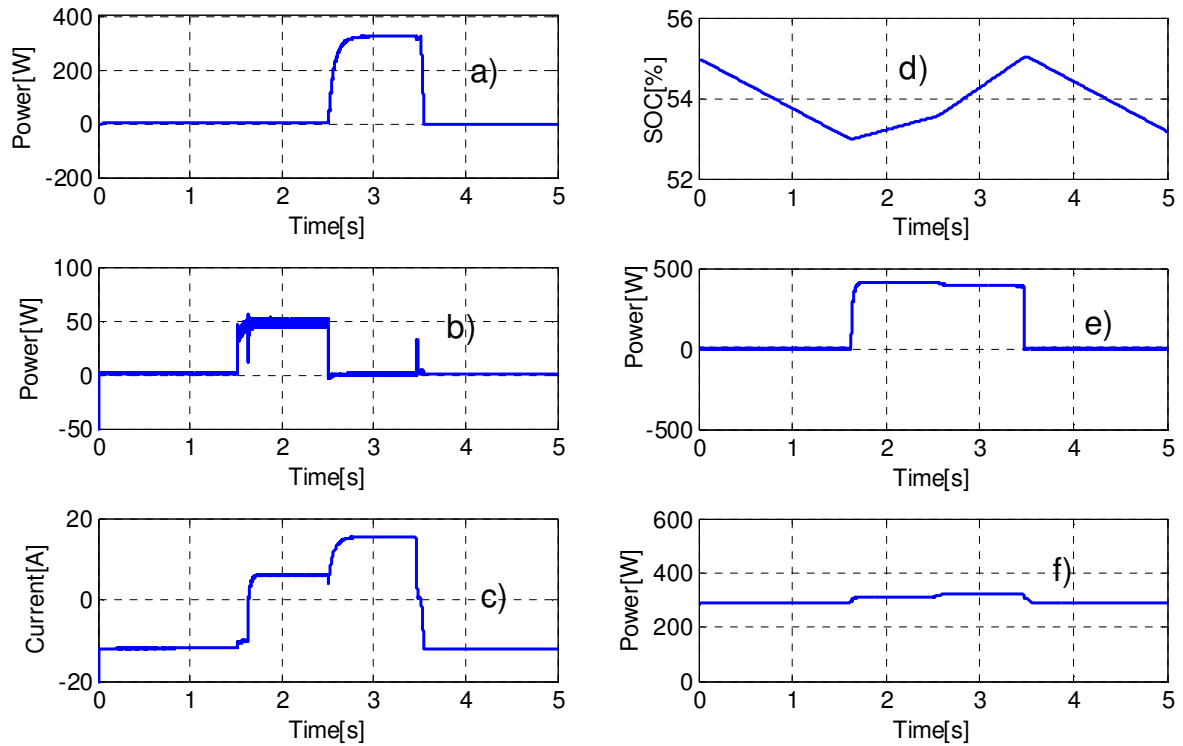

Figure 55. HPS response during the second case: (a) WECS power, (b) SPV power, (c) battery current, (d) battery SOC, e) BDG power and (f) load power

3.9 CONCLUSION

In this paper, a hybrid power system integrating three renewable energy sources including solar, wind and biodiesel as well as storage battery and DC load was presented. To efficiently extract maximum power from the solar panel and the wind turbine, fuzzy logic MPPT controller has been designed and implemented in these systems. In the aim of highlighting the performance of the FL MPPT controller, the simulations results of the SPV with FL technique were compared with P&O technique, and then the results of WECS with FL technique were compared to TSR technique. The analysis demonstrated that about 4 % performance is achieved with FL controller compared to P&O and TSR techniques. In addition, the coupling of the solar, wind and biodiesel systems was performed and analyzed through two cases. The two cases have demonstrated that coupling three different energy sources with one source working as backup permits to meet the load requirement under all-weather variation condition.

3.10 REFERENCES

[1]   Y.-H. Liu, C.-L. Liu, J.-W. Huang, and J.-H. Chen, "Neural-network-based maximum power point tracking methods for photovoltaic systems operating under fast changing environments," *Solar Energy,* vol. 89, pp. 42-53, 2013 2012.

[2]   J.-A. Jiang, T.-L. Huang, and Y.-T Hsiao. H.-H. Chen, "Maximum Power Tracking for Photovoltaic Power Systems," *Tamkang Journal of Science and Engineering, Vol. 8, No 2, pp. 147-153,* 2005.

[3]   T. Jacob and A. S, "Modeling of hybrid wind and photovoltaic energy system using a new converter topology," *Electrical and Electronics Engineering: An International Journal (EEEIJ) Vol.1, pp. 1-13, No.2,* 2012.

[4]   S. Alsadi and B. Alsayid, "Maximum Power Point Tracking Simulation for Photovoltaic Systems Using Perturb and Observe Algorithm," *International Journal of Engineering and Innovative Technology (IJEIT) Volume 2, Issue 6, pp. 80-85,* 2012.

[5]   M. Azouz, A. Shaltout, and M. A. L. Elshafei, "Fuzzy Logic Control of Wind Energy Systems," *Proceedings of the 14th International Middle East Power Systems Conference (MEPCON'10),* 2010.

[6]   M.-F. Tsai, C.-S. Tseng, and Y.-H. Hung, "A novel MPPT control design for wind-turbine generation systems using neural network compensator," in *IECON 2012-38th Annual Conference on IEEE Industrial Electronics Society*, 2012, pp. 3521-3526.

[7]   M. A. Abdullah, A. H. M. Yatim, and C. W. Tan, "A study of maximum power point tracking algorithms for wind energy system," *IEEE First Conference on Clean Energy and Technology CET,* pp. 321 - 326, 2011.

[8]   R. Ramaprabha, V. Gothandaraman, K. Kanimozhi, R. Divya, and B. L. Mathur, "Maximum Power Point Tracking using GA-Optimized Artificial Neural Network for Solar PV System," *1st International Conference on Electrical Energy Systems,* 2011.

[9]   G. F. T. Kebir, T. Obeidi, A. Ilinca, C. Larbes, and D. Ramdenee, "Design and Simulation of a New, High Performance Fuzzy MPPT Solar Energy System," 2014.

[10]   T. Shanthi and A.S. Vanmukhil, "Fuzzy Logic based MPPT Control of Hybrid Power Generation System," *International Journal of Computer Applications,* vol. 86, pp. 37-44, 2014.

[11]   T. Balamurugan and S. Manoharan, "Fuzzy Controller Design using Soft Switching Boost Converter for MPPT in Hybrid System," *International Journal of Soft Computing and Engineering (IJSCE)*, vol. 2, pp. 87-94, 2012.

[12]   F. Chekired, C. Larbes, D. Rekioua, and F. Haddad, "Implementation of a MPPT fuzzy controller for photovoltaic systems on FPGA circuit," *Energy Procedia,* vol. 6, pp. 541–549, 2011.

[13]   B. Bendiba, F. Krimb, H. Belmilia, M. F. Almia, and S. Bouloumaa, "Advanced Fuzzy MPPT Controller for a stand-alone PV system," *Energy Procedia,* vol. 50, pp. 383 – 392, 2014.

[14]   R. Boukenoui, H. Salhi, R. Bradai, and A. Mellit, "A new intelligent MPPT method for stand-alone photovoltaic systems operating under fast transient variations of shading patterns," *Solar Energy,* vol. 124, pp. 124–142, 2015.

CONCLUSION GÉNÉRALE

L'objectif de ce projet de recherche était d'étudier par modélisation et simulation le fonctionnement et le contrôle optimal d'un système hybride d'énergies renouvelables destiné à un laboratoire éducationnel permettant d'enseigner les étudiants les technologies des énergies renouvelables. Ce système hybride est composé d'un système de conversion d'énergie éolienne, d'un système solaire photovoltaïque, d'une génératrice au biodiesel, de contrôleurs de suivi du point de puissance maximale, de batteries de stockage et de charges. Pour ce faire, nous avons organisé notre travail suivant trois étapes qui ont permis de produire trois articles : (i) présentation du concept du laboratoire d'énergie renouvelable avec ses composants, leur analyse et leur dimensionnement, (ii) étude et simulation du système hybride en utilisant le contrôleur MPPT de type Perturber et Observer (P&O) et de type Contrôle de vitesse spécifique (TSR) pour l'extraction des puissances maximales du panneau solaire et de la turbine éolienne respectivement, et (iii) amélioration de l'efficacité et de la production du panneau solaire et de la turbine éolienne en utilisant des contrôleurs intelligents basés sur la logique floue.

Dans la première étape, le choix des types et le dimensionnement des capacités des différents composants du système hybride ont été effectués. Le fonctionnement du panneau solaire et de la turbine éolienne a été analysé suivant les variations des radiations solaires, de la vitesse du vent et des charges. Le système de la génératrice au biodiesel a également été présenté et étudié. Pour le panneau solaire, les caractéristiques puissance-tension (P¬V) et courant-tension (I¬V) avec les variations des radiations solaires et de la température ont été présentés. Ensuite, le panneau a été connecté directement à la batterie et à la charge sans régulateur et l'évolution des courants du panneau solaire, de la batterie et de la charge a été

analysée avec une variation de la charge et des radiations solaires. Pour l'éolienne, les caractéristiques du coefficient de puissance (C_P) versus la vitesse spécifique et de la puissance mécanique versus la vitesse du rotor ont été présentées. Pour étudier le fonctionnement de l'éolienne, celle-ci a été connectée directement à la batterie et à la charge puis l'évolution des courants de la turbine, de la batterie et de la charge a été analysée suivant les variations de la vitesse du vent et de la charge. Pour le système de la génératrice au biodiesel, l'évolution des courants de la génératrice, de la batterie et de la charge a été analysée suivant une variation de la charge. Après l'étude des trois sources séparément, elles ont été couplées en débitant sur une batterie et une charge commune. Cette étude a permis de montrer qu'avec le système de trois sources et une batterie, la charge est toujours suffisamment alimentée. Par ailleurs, le concept, l'architecture et l'environnement physique et virtuel du laboratoire ont été présentés dans cette étape avec tous les composants physiques et virtuels qui y sont intégrés.

Dans la deuxième étape, la modélisation du système de conversion d'énergie éolienne et du système solaire photovoltaïque, incluant leurs systèmes de contrôle optimal, a été effectué à l'aide des équations mathématiques qui régissent ces systèmes; ensuite, les modèles établis ont été simulés et analysée en utilisant le logiciel Matlab/Simulink. Des contrôleurs de type MPPT classiques ont étudiés et utilisés au niveau de ces deux systèmes pour l'extraction de la puissance maximale malgré la variation des radiations solaires et de la vitesse du vent. Pour cela, l'algorithme de contrôle Perturber et Observer (P&O) a été utilisé au niveau du système solaire photovoltaïque, tandis le contrôle de la vitesse spécifique (Tip Speed Ratio : TSR) a été adopté pour l'éolienne. Il a été démontré que ces contrôleurs permettaient effectivement de maintenir le panneau solaire et l'éolienne à leurs points de fonctionnement maximaux. Le système de la génératrice au biodiesel a aussi été brièvement présenté et analysé. Après l'étude séparée des trois sources, la stratégie de couplage des sources d'énergie a été démontrée, puis le système hybride complet a été analysé avec des scenarios suivant les variations des radiations solaires et des vitesses de

vent. L'étude a démontré que le système hybride mis au point permet d'assurer la fiabilité énergétique dans la mesure où la génératrice au biodiesel démarre dans le pire des scénarios lorsque l'énergie produite par le système solaire et l'éolienne n'est pas suffisante pour alimenter la charge et que la batterie est sous un seuil minimal de charge.

Dans la dernière étape, les techniques traditionnelles d'extraction des puissances maximales (commande MPPT) du panneau solaire et de l'éolienne ont été améliorées en remplaçant les contrôleurs P&O et TSR par des contrôleurs intelligents de logique floue. Ainsi, la théorie de la logique floue a été d'abord effectuée; ensuite, les systèmes de contrôle ont été développés pour le système solaire et le système éolien. Pour une meilleure analyse des performances, des comparaisons des résultats de simulations ont été effectuées pour le système solaire entre la commande MPPT de type logique floue et celle de type P&O et pour le système éolien entre la commande MPPT floue et celle de type TSR. L'étude a permis de s'apercevoir qu'avec la commande MPPT de type P&O, la puissance oscille beaucoup autour de la puissance maximale, alors qu'avec la commande MPPT floue, la puissance est plus stable. Dans l'éolienne, on se rend compte qu'avec les deux types de commandes MPPT, la puissance est presque similaire. Cependant, avec la commande MPPT floue, le coefficient de puissance et la puissance électrique obtenue sont environ 4 % supérieurs en comparaison avec la commande MPPT de type TSR, surtout lors de grands changements de vitesse de vent. Il ressort de cette étude que le contrôleur flou est plus précis que le contrôleur TSR en particulier lors de variations brusques de la vitesse du vent.

La suite logique de ce projet est de procéder au montage physique du laboratoire à l'Université du Québec à Rimouski et faire l'expérimentation du système hybride proposé. La théorie sur l'énergie éolienne, l'énergie solaire, la génératrice au biodiesel, les systèmes de commande MPPT et l'électronique de puissance sont entre autres des sujets qui seront traités dans le laboratoire. Un partenariat de jumelage entre l'UQAR et certains CÉGEPs

peut également être réalisé dans le cadre de ce projet en vue de favoriser l'enseignement des énergies renouvelables. Les étudiants pourront apprendre davantage sur tous les aspects liés aux technologies des énergies renouvelables et faire des séances de laboratoire sur site ou à distance. Ce projet se veut un cadre idéal de regroupement d'acteurs de disciplines diverses pour la promotion des énergies renouvelables partout dans le monde.